Alexandria Engineering Journal (2022) 61, 5753–5769

HOSTED BY

ELSEVIER

Alexandria University

Alexandria Engineering Journal

www.elsevier.com/locate/aej
www.sciencedirect.com

A novel analytical algorithm for generalized fifth-order time-fractional nonlinear evolution equations with conformable time derivative arising in shallow water waves

Omar Abu Arqub [a,b], Mohammed Al-Smadi [c,d], Hassan Almusawa [e], Dumitru Baleanu [f,g,h,*], Tasawar Hayat [b,i], Mohammed Alhodaly [b], M.S. Osman [j,]**

[a] *Department of Mathematics, Faculty of Science, Al Balqa Applied University, Salt 19117, Jordan*
[b] *Nonlinear Analysis and Applied Mathematics (NAAM) Research Group, Department of Mathematics, Faculty of Science, King Abdulaziz University, Jeddah 21589, Saudi Arabia*
[c] *Department of Applied Science, Ajloun College, Al-Balqa Applied University, Ajloun 26816, Jordan*
[d] *Nonlinear Dynamics Research Center (NDRC), Ajman University, Ajman, UAE*
[e] *Department of Mathematics, College of Sciences, Jazan University, Jazan 45142, Saudi Arabia*
[f] *Department of Mathematics, Faculty of Arts and Sciences, Cankaya University, Ogretmenler Cad. 1406530, Ankara, Turkey*
[g] *Institute of Space Sciences, Magurele, Bucharest, Romania*
[h] *Department of Medical Research, China Medical University Hospita, China Medical University, Taichung, Taiwan*
[i] *Department of Mathematics, Faculty of Science, Quaid-I-Azam University, Islamabad 45320, Pakistan*
[j] *Department of Mathematics, Faculty of Science, Cairo University, Giza 12613, Egypt*

Received 11 June 2021; revised 6 December 2021; accepted 16 December 2021
Available online 30 December 2021

KEYWORDS

Fractional nonlinear evolution equation;
Fractional conformable Korteweg-de Vries equations;
Fractional conformable derivative;

Abstract The purpose of this research is to study, investigate, and analyze a class of temporal time-FNEE models with time-FCDs that are indispensable in numerous nonlinear wave propagation phenomena. For this purpose, an efficient semi-analytical algorithm is developed and designed in view of the residual error terms for solving a class of fifth-order time-FCKdVEs. The analytical solutions of a dynamic wavefunction of the fractional Ito, Sawada-Kotera, Lax's Korteweg-de Vries, Caudrey-Dodd-Gibbon, and Kaup-Kupershmidt equations are provided in the form of a convergent conformable time-fractional series. The related consequences are discussed both theoret-

Abbreviations: OHAM, Optimal homotopy asymptotic method; q-HAM, q-homotopy analysis method; HPM, Homotopy perturbation method; BPM, Bernstein polynomials method; LMM, Legendre multiwavelet method; ADM, Adomian decomposition method; VIM, Variational iteration method; FCD, Fractional conformable derivative; FCRPSA, Fractional conformable residual power series algorithm; FNEE, Fractional nonlinear evolution equation; FPDE, Fractional partial differential equation; FCKdVE, Fractional conformable Korteweg-de Vries equations; MTFS, multiple time-fractional series

* Corresponding author at: Department of Mathematics, Faculty of Arts and Sciences, Cankaya University, Ogretmenler Cad. 1406530, Ankara, Turkey.
** Corresponding author at: Department of Mathematics, Faculty of Science, Cairo University, Giza 12613, Egypt.
E-mail addresses: dumitru@cankaya.edu.tr (D. Baleanu), mofatzi@cu.edu.eg, mofatzi@sci.cu.edu.eg (M.S. Osman).

Peer review under responsibility of Faculty of Engineering, Alexandria University.

https://doi.org/10.1016/j.aej.2021.12.044

Fractional conformable residual power series algorithm;
Shallow water surfaces

ically as well as numerically considering the conformable sense. In this direction, convergence analysis and error estimates of the developed algorithm are studied and analyzed as well. Concerning the considered models, specific unidirectional physical experiments are given in a finite compact regime to confirm the theoretical aspects and to demonstrate the superiority of the novel algorithm compared to the other existing numerical methods. Moreover, some representative results are presented in two- and three-dimensional graphs, whilst dynamic behaviors of fractional parameters are reported for several α values. From the practical viewpoint, the archived simulations and consequences justify that the iterative algorithm is a straightforward and appropriate tool with computational efficiency for long-wavelength solutions of nonlinear time-FPDEs in physical phenomena.

1. Introduction

The time-FNEE is a mathematical dynamic system suitable for long wave propagation solutions of nonlinear dispersive time-FPDEs playing a significant role in balancing the dispersion and nonlinearity effects of soliton behavior [1-4]. The application of such FNEE models can be found in different branches of pure and applied sciences, including capillary gravity waves, soliton theory, meteorology, hydrodynamics, the surface tension of shallow-water waves, and incompressible and inviscid fluid [3-7]. On the other aspect as well, time-FPDEs play a critical role in modeling and studying complex nonlinear systems, and in understanding the basic physics, interactions of elementary particles, and dynamic processes that govern these systems. It has recently attracted the attention of scientists due to its tremendous applications in various scientific fields such as quantum mechanics, chemical kinetics, electromagnetic, control theory, magneto-acoustic propagation in plasma, dissipative systems, hydrodynamics, granular fluids, and gas–solid flows [8-13]. Various types of time-FNEEs have been derived in the literature, where some of them do not admit N-soliton solutions [14]. Meanwhile, different kinds of both local and nonlocal fractional concepts have been refined and modified like Riesz-Caputo, Atangana-Baleanu, Caputo-Katugampola, Machado, Hilfer-Hadamard, Grünwald-Letnikov, Erdelyi-Kober, Riemann-Liouville, and FCD. Although the nonlocal fractional concept is more interesting due to the long-term physical features relies on memory and nonlocality effects, there is also a deficiency elsewhere such as chain, Leibniz, quotient, and semi-group properties. In this orientation, local fractional derivatives rely on the natural generalization of standard derivatives of a non-integer power to conserve the local nature of the derivatives, eschew fracturing the extraordinary rules, and inspect the scaling features of local asymptotic [15-21].

So far, effective reliable semi-analytical techniques and numerical approaches are successfully developed and applied for dealing with various categories of time-FNEEs, including OHAM, HPM, BPM, LMM, ADM, VIM, and reproducing kernel method. Moreover, many traveling waves concepts like modified Kudryashov method, tanh-sech method, wavelet transform method, Riccati sub-equation method, G'/G-expansion method, sine-Gordon expansion method, and other methods [22-39]. Finding exact and approximate soliton solutions of higher-order time-FPDEs in wave propagation situations is a significant issue to understand the dynamic behaviors of nonlinear waves in dispersive media. For this purpose, we intend in this work to create accurate approximate solutions of FNEEs in FCD sense subject to suitable initial conditions utilizing a novel analytical algorithm. The primary motivation for implementing this algorithm is to achieve effective approximate solutions straightforwardly without imposing any undue restrictions on the model nature and gaining rapid convergence with the lower cost of calculations. The following is a well-known model for the temporal time-FNEE [22,23]:

$$\frac{\partial^{\alpha} \upsilon}{\partial t} + p\upsilon^{2}\frac{\partial \upsilon}{\partial x} + q\frac{\partial \upsilon}{\partial x}\frac{\partial^{2} \upsilon}{\partial x^{2}} + r\upsilon\frac{\partial^{3} \upsilon}{\partial x^{3}} + \frac{\partial^{5} \upsilon}{\partial x^{5}} = 0, \tag{1}$$

where $0 < \alpha \leq 1$, p, q, r are nontrivial constant parameters, α stands for the order of fractional time-dependent derivative, and $\upsilon = \upsilon(x, t)$ is the surface wave elevation of a liquid in the dispersive media in terms of the space $x \in [a, b]$ and time $t \geq 0$ coordinates. Typically, model (1) consists of three nonlinear terms and a linear dispersive term $\partial^{5}\upsilon/\partial x^{5}$ so it plays a significant role in balancing the dispersion and nonlinearity effects of soliton behavior [1]. The proposed model is profitably used in many physical applications in nonlinear wave propagation phenomena such as surface tension of shallow water, acoustic magnetic propagation in plasma, gravitational field, incompressible and inviscid fluids, etc [9,22]. By taking different process values of p, q and r a varied version of the time-FNEEs can be formulated as follows:

- Taking $p = 2$, $q = 6$, and $r = 3$, we get the fractional Ito equation [23,24]as

$$\frac{\partial^{\alpha} \upsilon}{\partial t} + 2\upsilon^{2}\frac{\partial \upsilon}{\partial x} + 6\frac{\partial \upsilon}{\partial x}\frac{\partial^{2} \upsilon}{\partial x^{2}} + 3\upsilon\frac{\partial^{3} \upsilon}{\partial x^{3}} + \frac{\partial^{5} \upsilon}{\partial x^{5}} = 0. \tag{2}$$

- Taking $p = 45$ and $q = r = 15$, we get the fractional Sawada-Kotera equation [23,27] as

$$\frac{\partial^{\alpha} \upsilon}{\partial t} + 45\upsilon^{2}\frac{\partial \upsilon}{\partial x} + 15\frac{\partial \upsilon}{\partial x}\frac{\partial^{2} \upsilon}{\partial x^{2}} + 15\upsilon\frac{\partial^{3} \upsilon}{\partial x^{3}} + \frac{\partial^{5} \upsilon}{\partial x^{5}} = 0. \tag{3}$$

- Taking $p = q = 30$ and $r = 15$, we get the fractional Lax's Korteweg-de Vries equation [5,40] as

$$\frac{\partial^{\alpha} \upsilon}{\partial t} + 30\upsilon^{2}\frac{\partial \upsilon}{\partial x} + 30\frac{\partial \upsilon}{\partial x}\frac{\partial^{2} \upsilon}{\partial x^{2}} + 10\upsilon\frac{\partial^{3} \upsilon}{\partial x^{3}} + \frac{\partial^{5} \upsilon}{\partial x^{5}} = 0. \tag{4}$$

- Taking $p = 180$ and $q = r = 30$, we get the fractional Caudrey-Dodd-Gibbon equation [40,41] as

$$\frac{\partial^\alpha v}{\partial t} + 180v^2\frac{\partial v}{\partial x} + 30\frac{\partial v}{\partial x}\frac{\partial^2 v}{\partial x^2} + 30v\frac{\partial^3 v}{\partial x^3} + \frac{\partial^5 v}{\partial x^5} = 0. \quad (5)$$

- Taking $p = 45$ and $q = r = -15$, we get the fractional Kaup-Kupershmidt equation [14,42] as

$$\frac{\partial^\alpha v}{\partial t} + 45v^2\frac{\partial v}{\partial x} - 15\frac{\partial v}{\partial x}\frac{\partial^2 v}{\partial x^2} - 15v\frac{\partial^3 v}{\partial x^3} + \frac{\partial^5 v}{\partial x^5} = 0. \quad (6)$$

Hereinafter, the aforementioned time-FCKdVEs (2–6) are equipped with the underlying initial condition:

$$v(x,0) = v_0(x), \quad (7)$$

where $x \in [a, b]$, $v_0(x)$ is a sufficiently smooth bounded function.

The FCKdVE models have been profitably used for modeling the nonlinear dispersive waves phenomena that occurring in capillary waves, nonlinear optics, scattering theory, Hamiltonian dynamics, plasma physics, gravitational fields, Bose-Einstein condensates, and atmospheric waves [22-24]. In [22], the time-fractional Sawada-Kotera equation was considered under the Caputo concept to investigate exact and multiple soliton solutions using the trial equation and Hirota's methods and to approximate soliton solutions using the FCRPSA. Using the G''/G-expansion method [27] exact traveling wave solutions of nonlinear time-FNEEs have been successfully obtained. Moreover, new sets of exact traveling wave solutions for time-fractional Caudrey-Dodd-Gibbon-Sawada-Kotera equation in terms of the Riemann-Liouville concept were attained in [9] along with a discussion of conservation laws. In [28], tanh-sech and modified Kudryashov methods have been used to solve the fractional modified Sawada-Kotera equation using a local fractional derivative. Further, the time-fractional Sawada-Kotera and Ito equations have been numerically solved considering Caputo sense based on BPM [24]. Gupta and Ray [42] effectively studied approximate solutions of the time-fractional Kaup-Kupershmidt equation employing LMM and OHAM. By employing the q-HAM [23], approximate solutions of fractional Ito and Sawada-Kotera equations have been successfully obtained.

Typically, there is no conventional approach that produces an analytical prototype solution, soliton solution, or closed-form traveling wave solutions for nonlinear dispersive FPDEs. Hence, there is an urgent need for reliable and sophisticated techniques to explore analytical and numerical solutions to these equations. Motivated by the aforementioned argumentations, this paper aims to design an advanced iterative algorithm, so-called, the FCRPSA for generating analytical solutions of nonlinear time-FCKdVE models by utilizing a new fractional index in light of the FCD sense. Error estimates and convergence analysis for the present FCRPSA are discussed as well. The relevant theoretical results are affirmed by numerical simulations. Eventually, five-types numerical examples are tested to verify the efficiency of the novel fractional algorithm, including the time-fractional Ito, Sawada-Kotera, Lax's Korteweg-de Vries, Caudrey-Dodd-Gibbon, and Kaup-Kupershmidt equations.

The rest of the paper is arranged as follows. Hereinafter, some primary definitions and theorems are briefly retrieved. In Section 3, an efficient analytical FCRPSA is extended to solve nonlinear FCKdVE of the fifth order. Specific numerical applications are stated in Section 4 to support the theoretical aspect. Meanwhile, numerical consequences, discussions, and physical explanations are reported followed by some deducing remarks in Section 5.

2. Preliminary results and definitions

Fractional calculus shows up in different fields of pure and applied physics, biology, chemistry, and engineering as excellent mathematical tools to describe the memory and hereditary characteristics of many materials and processes [43-55]. It was used to formulate several nonlinear time-FPDE schemes with merit given to suppling a more comprehensive discussion of chaos, dynamic systems, and the pattern of state change over time.

In this direction, different fractional operators have been investigated in the literature to handle such equations as Riesz derivative, Riemann-Liouville derivative, Caputo derivative, Feller derivative, Grünwald derivative, Caputo-Fabrizio derivative, Atangana-Baleanu derivative, and local fractional derivative [17-21]. Consequently, the FCD was modified based on the general standard notion of limits [56]. This part is purposed to highlight the main definition of FCD with its characteristics. Moreover, a summary of the series expansion in the FCD sense is stated.

Definition 1 ([56]). *The α th order FCD of $v(t) : [0,\infty) \to \mathbb{R}$ for $\alpha \in (0,1)$ is defined as*

$$\frac{\partial^\alpha v(t)}{\partial t} = \lim_{\varepsilon\to 0} \frac{v\left(t + \varepsilon t^{1-\alpha}\right) - v(t)}{\varepsilon}, t > 0. \quad (8)$$

Moreover, if the previous limit exists at a point $s, s > 0$ in $(0, s)$, then $v(t)$ is called α-differentiable so that $\partial^\alpha v(s)/\partial t = \lim_{t\to s^+} \partial^\alpha v(t)/\partial t$.

Definition 2 ([57]). *Let $v(t) : [s,\infty) \to \mathbb{R}$ be α-differentiable. The α-fractional integral starting from s is defined as*

$$\mathcal{I}^\alpha_s v(t) = \int_s^t \frac{v(\xi)}{\xi^{1-\alpha}} d\xi, t > s \geq 0, \quad (9)$$

in which $\alpha \in (0,1]$ and the integral represents the usual Riemann improper integral.

In the following, we present some interesting properties acquired in terms of FCD [57]. Further features can be found in [58-69] and the references therein.

Lemma 1 ([57]). *Let $v(t)$ and $u(t)$ be α-differentiable functions at any point $t > 0$. Then, we have the following properties:*

- $\frac{\partial^\alpha}{\partial t} v(t) = t^{1-\alpha} \frac{\partial}{\partial t} v(t)$.
- $\frac{\partial^\alpha}{\partial t}(c_1 v(t) + c_2 u(t)) = c_1 \frac{\partial^\alpha}{\partial t} v(t) + c_2 \frac{\partial^\alpha}{\partial t} u(t)$, where c_1 and c_2 are real constants.
- $\frac{\partial^\alpha}{\partial t}\left(t^k\right) = k t^{k-\alpha}$, where k is an arbitrary constant.
- $\frac{\partial^\alpha}{\partial t}(\mathcal{C}) = 0$, where $\mathcal{C}$ is a constant.

- $\frac{\partial^\alpha}{\partial t}[v(t)u(t)] = v(t)\frac{\partial^\alpha}{\partial t}u(t) + u(t)\frac{\partial^\alpha}{\partial t}v(t)$.
- $\frac{\partial^\alpha}{\partial t}[v(t)/u(t)] = \left(u(t)\frac{\partial^\alpha}{\partial t}v(t) - v(t)\frac{\partial^\alpha}{\partial t}u(t)\right)/u^2(t)$, where $u(t)$ is a nonzero function.

Theorem 1 (*[57]*). *Suppose that $v : (0,\infty) \to \mathbb{R}$ is a differentiable and α-differentiable function, while $u(t)$ is a differentiable function defined on the range of $v(t)$. Then, the α-differentiable chain rule of the composition of the two functions for $\alpha \in (0,1]$ is provided as*

$$\frac{\partial^\alpha (v^\circ u)(t)}{\partial t} = t^{1-\alpha}u'(t)v'(u(t)). \tag{10}$$

Definition 3 (*[58]*). *For $\alpha \in (0,1]$, let v be a function of x and t defined on $[a,b]\times[s,\infty)$ to $\mathbb{R}$. Then, the time-FCD of order α is given as*

$$\frac{\partial^\alpha}{\partial t}v(x,t) = \lim_{\varepsilon\to 0}\frac{v\left(x, t+\varepsilon(t-s)^{1-\alpha}\right) - v(x,t)}{\varepsilon}. \tag{11}$$

Definition 4 (*[58]*). *For $\alpha \in (0,1]$, let v be a function of x and t defined on $[a,b]\times[s,\infty)$ to $\mathbb{R}$. Then, the conformable fractional integral starting from s of order α is given as*

$$\mathscr{I}^\alpha_s v(x,t) = \int_s^t \frac{v(x,\xi)}{(\xi - s)^{1-\alpha}}d\xi. \tag{12}$$

Definition 5 (*[11]*). *The MTFS about $t_0 > 0$ is given as*

$$\sum_{i=0}^{\infty}\mathscr{C}_i(x)(t-t_0)^{i\alpha} = \mathscr{C}_0(x) + \mathscr{C}_1(x)(t-t_0)^\alpha + \mathscr{C}_2(x)(t-t_0)^{2\alpha} + \cdots, \tag{13}$$

where $\in (n-1,n]$, $t \in \left[t_0, t_0 + r^{1/\alpha}\right), r > 0$, $r^{1/\alpha}$ is a radius of convergence, and $\mathscr{C}_i(x)$ indicates unknown coefficients of the MTFS expansion.

When $\alpha = 1$, then the MTFS expansion in Definition 5 reduces to the usual series expansion at $t_0 > 0$ with the radius of convergence r that converges uniformly on $|t - t_0| < r$.

Theorem 2 (*[11]*). *Let $v = v(x,t)$ be a function that has infinitely time-FCDs at any point t on $[t_0, t_0 + r^{1/\alpha})$ such that $v(x,t)$ has the following MTFS expansion about $t_0 > 0$*

$$v(x,t) = \sum_{i=0}^{\infty}\mathscr{C}_i(x)(t-t_0)^{i\alpha}, \alpha > 0. \tag{14}$$

Then, the coefficients $\mathscr{C}_i(x)$, $i = 0,1,2,\cdots$, are evaluated as

$$\mathscr{C}_i(x) = \frac{\partial^{i\alpha}_{t_0}v(x,t_0)}{i!\alpha^i}, \tag{15}$$

in which $\partial^{i\alpha}_{t_0}v(x,t_0)$ indicates the i th time-FCD of $v(x,t)$ at $t_0 > 0$ such that $\partial^{i\alpha}_{t_0}v(x,t_0) = \partial^\alpha_{t_0}.\partial^\alpha_{t_0}\cdots\partial^\alpha_{t_0}v(x,t_0)$ (i-times).

3. The FCRPSA: construction, steps, and analysis

The FCRPSA is a semi-approximate concept specifically introduced for solving complex nonlinear time-FPDEs arising in different categories of science. This technique is instituted on generalizing the expansion of the Taylor series for arbitrary order and minimizing the residual errors identified to detect the unknown compounds, which was proposed and developed by Abu Arqub in the study of fuzzy differential equations. It has many motivational and attractive aspects, in addition to a massive ability to solve the nonlinear terms directly without requiring any restrictions, transformation, linearization, or perturbation on the configuration of the models. Thus, it has acquired a lot of consideration and has become an energizing focus of the research community [56-69].

In this segment, a newly developed algorithm is designed to obtain accurate approximate solutions of the time-FCKdVE models equipped with a certain initial condition within a finite spatiotemporal domain. To reach our aim, let us consider the nonlinear time-FCKdVE as follows:

$$\partial^\alpha_t v(x,t) + \mathscr{N}\left(v, v^2, v_x, v_{2x}, v_{3x}\right) + v_{5x}(x,t) = 0, \tag{16}$$

along with the underlying initial condition

$$v(x,0) = v_0(x), \tag{17}$$

where $0 < \alpha \le 1$, $x \in [a,b]$, $t \ge 0$, α is the FCD parameter, $v_{ix} = \partial^i v(x,t)/\partial x^i$, $i = 1,2,3$, $v_0(x)$ is a given bounded function, and $v(x,t)$ is a sufficiently smooth wavefunction. Herein, $\mathscr{N}$ indicates the nonlinear operator in terms of $v^2 v_x$, $v_x v_{2x}$ and $v v_{3x}$ over a space–time domain.

The presented FCRPSA assumes that the solution $v(x,t)$ of (16–17) has an MTFS expansion of about $t_0 = 0$ of the following form:

$$v(x,t) = \sum_{i=0}^{\infty}\mathscr{C}_i(x)\frac{t^{i\alpha}}{i!\alpha^i}, \tag{18}$$

provided that $v(x,0) = \mathscr{C}_0(x) = v_0(x)$. Therefore, the m-term truncated series solution $v_m(x,t)$ of $v(x,t)$ in view of (17) can be expressed by

$$v_m(x,t) = \mathscr{C}_0(x) + \sum_{i=1}^{m}\mathscr{C}_i(x)\frac{t^{i\alpha}}{i!\alpha^i}. \tag{19}$$

Initially, the residual error $\mathscr{R}_s(x,t)$ of (16–17) is given by

$$\mathscr{R}_s(x,t) = \partial^\alpha_t v(x,t) + \mathscr{N}\left(v, v^2, v_x, v_{2x}, v_{3x}\right) + v_{5x}(x,t), \tag{20}$$

and then the m-term truncated residual of $\mathscr{R}_s(x,t)$ is given by

$$\mathscr{R}^m_s(x,t) = \partial^\alpha_t v_m(x,t) + \mathscr{N}\left(v_m, v_m^2, v_{x,m}, v_{2x,m}, v_{3x,m}\right) + v_{5x,m}, \tag{21}$$

where $v_{kx,m} = \partial^k v_m(x,t)/\partial_{x^k}$, $\mathscr{R}_s(x,t) = 0 = \partial^{(m-1)\alpha}\mathscr{R}_s/\partial t$, $m = 1,2,3,\cdots, x \in [a,b]$, $0 \le t < \mathscr{T}$, $\mathscr{T} \equiv t_0 + r^{1/\alpha}$, and $\partial^{(m-1)\alpha}\mathscr{R}^m_s/\partial t_{|t=0} \equiv 0$ for each $m = 1,2,3,\cdots$.

To clarify the main steps of the presented FCRPSA in finding the unknown coefficients $\mathscr{C}_i(x)$ of the m-term truncated solution (19), set $m = 1$ and equate $\mathscr{R}^1_s(x,t)$ to zero at $t = 0$. So, $\mathscr{C}_1(x)$ is obtained. Thereafter, set $m = 2$, apply the operator ∂^α_t on both sides of the resulting relevant equation, and solve $\partial_t^{\alpha}\mathscr{R}_{\jmath}^2(x,0)=0$. Then, $\mathscr{C}_2(x)$ is obtained as well. If we continued in this fashion, the unknown coefficients $\mathscr{C}_i(x)$, $i\geq 3$, of the MTFS expansion (19) will be obtained. For further clarification, the following algorithm is devoted.

Algorithm 1. *Finding the m th approximation of the solution of nonlinear time-FCKdVE* (16–17).

Step A. Let the solution $v(x,t)$ of (16–17) can be expanded about $t_0=0$ as

$$v(x,t)=\sum_{i=0}^{\infty}\mathscr{C}_i(x)\frac{t^{i\alpha}}{i!\alpha^i},\ t\geq t_0. \tag{22}$$

Step B. Define the m th-truncated solution of $v(x,t)$ in view of (17) as

$$v_m(x,t)=\mathscr{C}_0(x)+\sum_{i=1}^{m}\mathscr{C}_i(x)\frac{t^{i\alpha}}{i!\alpha^i}. \tag{23}$$

Step C. Truncate the m th residual error of $\mathscr{R}_{\jmath}(x,t)$ such that

$$\begin{aligned}\mathscr{R}_{\jmath}^m(x,t)&=\partial_t^{\alpha}v_m(x,t)+\mathscr{N}\left(v_m,v_m^2,v_{x,m},v_{2x,m},v_{3x,m}\right)\\&\quad+v_{5x,m},v_{kx,m}.\end{aligned} \tag{24}$$

Step D. Substitute the truncated MTFS solution in Step B to the m th-truncated residual error in Step C as

$$\begin{aligned}\mathscr{R}_{\jmath}^m(x,t)&=\partial_t^{\alpha}\left(\mathscr{C}_0(x)+\sum_{i=1}^{m}\mathscr{C}_i(x)\frac{t^{i\alpha}}{i!\alpha^i}\right)\\&\quad+\left(\mathscr{C}_0(x)+\sum_{i=1}^{m}\mathscr{C}_i(x)\frac{t^{i\alpha}}{i!\alpha^i}\right)_{5x}\\&\quad+\mathscr{N}\left[\left(\mathscr{C}_0(x)+\sum_{i=1}^{m}\mathscr{C}_i(x)\frac{t^{i\alpha}}{i!\alpha^i}\right),\right.\\&\quad\left(\mathscr{C}_0(x)+\sum_{i=1}^{m}\mathscr{C}_i(x)\frac{t^{i\alpha}}{i!\alpha^i}\right)^2,\cdots,\\&\quad\left.\left(\mathscr{C}_0(x)+\sum_{i=1}^{m}\mathscr{C}_i(x)\frac{t^{i\alpha}}{i!\alpha^i}\right)_{3x}\right].\end{aligned} \tag{25}$$

Step E. Apply the operator $\partial_t^{(m-1)\alpha}$ for each $m=1,2,3,\cdots$ on both sides of the resulting equation in Step D as

$$\begin{aligned}\partial_t^{(m-1)\alpha}\mathscr{R}_{\jmath}^m(x,t)&=\partial_t^{m\alpha}\left(\mathscr{C}_0(x)+\sum_{i=1}^{m}\mathscr{C}_i(x)\frac{t^{i\alpha}}{i!\alpha^i}\right)\\&\quad+\partial_t^{(m-1)\alpha}\left(\mathscr{C}_0(x)+\sum_{i=1}^{m}\mathscr{C}_i(x)\frac{t^{i\alpha}}{i!\alpha^i}\right)_{5x}\\&\quad+\partial_t^{(m-1)\alpha}\mathscr{N}\left[\left(\mathscr{C}_0(x)+\sum_{i=1}^{m}\mathscr{C}_i(x)\frac{t^{i\alpha}}{i!\alpha^i}\right),\right.\\&\quad\left(\mathscr{C}_0(x)+\sum_{i=1}^{m}\mathscr{C}_i(x)\frac{t^{i\alpha}}{i!\alpha^i}\right)^2,\cdots,\\&\quad\left.\left(\mathscr{C}_0(x)+\sum_{i=1}^{m}\mathscr{C}_i(x)\frac{t^{i\alpha}}{i!\alpha^i}\right)_{3x}\right].\end{aligned} \tag{26}$$

Step F. Execute the following subroutine to get the first few terms for the unknown coefficients $\mathscr{C}_i(x)$ with the help of $\partial_t^{(m-1)\alpha}\mathscr{R}_{\jmath}^m(x,0)=0$:

F1. Put $m=1$ in Step E, compute $\mathscr{R}_{\jmath}^1(x,t)$, and solve $\mathscr{R}_{\jmath}^1(x,0)=0$ to get $\mathscr{C}_1(x)$.

F2. Put $m=2$ in Step E, compute $\partial_t^{\alpha}\mathscr{R}_{\jmath}^2(x,t)$, and solve $\partial_t^{\alpha}\mathscr{R}_{\jmath}^2(x,0)=0$ to get $\mathscr{C}_2(x)$.

F3. Put $m=3$ in Step E, compute $\partial_t^{2\alpha}\mathscr{R}_{\jmath}^3(x,t)$, and solve $\partial_t^{2\alpha}\mathscr{R}_{\jmath}^3(x,0)=0$ to get $\mathscr{C}_3(x)$.

F4. Continue the procedure up to arbitrary order n by putting $m=n$, computing $\partial_t^{(n-1)\alpha}\mathscr{R}_{\jmath}^n(x,t)$, and solving the resulting equation $\partial_t^{(n-1)\alpha}\mathscr{R}_{\jmath}^n(x,0)=0$ to get the n th coefficients $\mathscr{C}_n(x)$.

Step G. Collect the gained components in the form of infinite series. Eventually, the closed-form of the solution can be obtained so that $v(x,t)=\lim_{n\to\infty}v_n(x,t)$ when the dynamical relation of the pattern is regular. Otherwise, the approximate solutions $v_n(x,t)$ can be obtained; Then, Stop.

Lemma 2. *Suppose that $v(x,t)$ is the solution of* (16–17)*, which has infinitely time-FCDs at any point t on $[t_0,t_0+r^{1/\alpha})$, and it can be expanded in the form of MTFS* (18) *about $t_0=0$. If there exists a positive function $\eta(x)>0$ such that $\left|\partial_t^{(m+1)\alpha}v(x,\xi)\right|\leq\eta(x)$ for all ξ between t and 0, then the remaining term of the MTFS expansion fulfills the following:*

$$|\mathscr{P}_n(x,t)|\leq\frac{\eta(x)}{(m+1)!\alpha^{m+1}}t^{(m+1)\alpha}, \tag{27}$$

in which $\mathscr{P}_n(x,t)=\sum_{n=m+1}^{\infty}\frac{\partial_t^{n\alpha}v(x,\xi)}{\alpha^n n!}t^{n\alpha}$.

Corollary 1. *Suppose that $v(x,t)$ and $v_m(x,t)$ are the analytical and approximate solutions of* (16–17)*, respectively. Let there exists a fixed constant $\lambda\in[0,1]$ such that $\|v_{m+1}(x,t)\|\leq\lambda\|v_m(x,t)\|$ for each $(x,t)\in[a,b]\times[t_0,\mathscr{T})$, and $\|\mathscr{C}_0(x)\|<\infty$ for each $x\in[a,b]$. Then, the approximate solution $v_m(x,t)$ converges to the analytical solution $v(x,t)$ whenever $m\to\infty$.*

Proof. Since $\|v_{m+1}(x,t)\|\leq\lambda\|v_m(x,t)\|$ for each $(x,t)\in[a,b]\times[t_0,\mathscr{T})$, then $\|v_1(x,t)\|\leq\lambda\|v_0(x,t)\|=\lambda\|\mathscr{C}_0(x)\|$, and then $\|v_2(x,t)\|\leq\lambda^2\|\mathscr{C}_0(x)\|$. Subsequently, we have $\|v_m(x,t)\|\leq\lambda^m\|\mathscr{C}_0(x)\|$. This leads to $\sum_{n=m+1}^{\infty}\|v_n(x,t)\|\leq\|\mathscr{C}_0(x)\|\sum_{n=m+1}^{\infty}\lambda^n$. Thus,

$$\begin{aligned}&\|v(x,t)-v_m(x,t)\|=\|\textstyle\sum_{n=m+1}^{\infty}v_n(x,t)\|\\&\leq\textstyle\sum_{n=m+1}^{\infty}\|v_n(x,t)\|\\&\leq\textstyle\sum_{n=m+1}^{\infty}\lambda^n\|\mathscr{C}_0(x)\|\\&=\tfrac{\lambda^{m+1}}{1-\lambda}\|\mathscr{C}_0(x)\|\\&\to 0\text{for}m\to\infty.\end{aligned} \tag{28}$$

4. Applications and simulation results

Temporal time-FNEEs are excellent tools for modeling nonlinear wave phenomena of dispersed media, and for understanding their dynamical behaviors. The higher-order time-FCKdVE is a unidirectional temporal nonlinear evolution model for describing the propagation of long and shallow water surface waves under capillary gravity [22-27]. It plays a significant role in balancing the dispersion and nonlinear effects of soliton behavior.

In this segment, the FCRPSA in light of the residual error functions is profitably applied for solving time-fractional Ito, Sawada-Kotera, Lax's Korteweg-de Vries, Caudrey-Dodd-Gibbon, and Kaup-Kupershmidt equations, which are the most popular species of fractional Korteweg-de Vries family hierarchy. Numerical simulation of these models is discussed and studied as well. Some graphical representative results are presented with physical interpretations for several fractional parameters to support the theoretical framework, and to give a clear visualization of the wavefunction behavior of the proposed models. Further, numerical comparisons are made to illustrate the effectiveness and simplicity of the presented FCRPSA. All calculations and representative results are performed by using the Mathematica computing system.

4.1. Application 1: Time-fractional Ito equation

In this portion, consider the fractional Ito equation with time-FCD in the underlying model [23,24]:

$$\frac{\partial^\alpha \upsilon}{\partial t}+2\upsilon^2\frac{\partial \upsilon}{\partial x}+6\frac{\partial \upsilon}{\partial x}\frac{\partial^2 \upsilon}{\partial x^2}+3\upsilon\frac{\partial^3 \upsilon}{\partial x^3}+\frac{\partial^5 \upsilon}{\partial x^5}=0, \tag{29}$$

associated with the underlying initial condition

$$\upsilon(x,0)=20\kappa^2-30\kappa^2\tanh^2(\kappa x), \tag{30}$$

where $0<\alpha\le 1$, κ is an arbitrary constant with $\kappa\neq 0$, $x\in[a,b]$, $t\ge 0$, and $\upsilon=\upsilon(x,t)$ is a sufficiently smooth function represented the elevation of wave surface of a liquid in the dispersed media. Typically, this equation consists of three nonlinear terms and one linear dispersive term $\partial^5\upsilon/\partial x^5$, which is not fully integrable but admits a limited range of conservation laws [1]. The fractional Ito equation is an indispensable model for numerous nonlinear physical applications in magneto-acoustic propagation in plasma, the surface tension of shallow water, hydrodynamics, etc. [2-7].

Utilizing the FCRPSA, the MTFS solution $\upsilon(x,t)$ of (29–30) about $t=0$ can be constructed as follows:

$$\upsilon(x,t)=\sum_{i=0}^{\infty}\mathscr{C}_i(x)\frac{t^{i\alpha}}{\alpha^i i!}, \tag{31}$$

in which $\mathscr{C}_0(x)=\upsilon(x,0)=20\kappa^2-30\kappa^2\tanh^2(\kappa x)$. Subsequently, the m-term truncated series $\upsilon_m(x,t)$ of $\upsilon(x,t)$ in view of (30) can be written as

$$\upsilon_m(x,t)=20\kappa^2-30\kappa^2\tanh^2(\kappa x)+\sum_{i=1}^{m}\mathscr{C}_i(x)\frac{t^{i\alpha}}{\alpha^i i!}. \tag{32}$$

Meanwhile, the residual error function $\mathscr{R}_s(x,t)$ can be written as

$$\mathscr{R}_s(x,t)=\frac{\partial^\alpha \upsilon}{\partial t}+2\upsilon^2\frac{\partial \upsilon}{\partial x}+6\frac{\partial \upsilon}{\partial x}\frac{\partial^2 \upsilon}{\partial x^2}+3\upsilon\frac{\partial^3 \upsilon}{\partial x^3}+\frac{\partial^5 \upsilon}{\partial x^5}, \tag{33}$$

provided that $\mathscr{R}_s(x,t)=0=\partial^{(m-1)\alpha}\mathscr{R}_s/\partial t$, $m=1,2,3,\cdots,x\in[a,b]$, and $0\le t<\mathscr{T}$.

In this direction as well, the m-term truncated residual $\mathscr{R}_s^m(x,t)$ of $\mathscr{R}_s(x,t)$ can be written as

$$\mathscr{R}_s^m(x,t)=\frac{\partial^\alpha \upsilon_m}{\partial t}+2\upsilon_m^2\frac{\partial \upsilon_m}{\partial x}+6\frac{\partial \upsilon_m}{\partial x}\frac{\partial^2 \upsilon_m}{\partial x^2}+3\upsilon_m\frac{\partial^3 \upsilon_m}{\partial x^3}+\frac{\partial^5 \upsilon_m}{\partial x^5}, \tag{34}$$

in which $\partial^{(m-1)\alpha}\mathscr{R}_s^m/\partial t_{|t=0}\equiv 0$ for each $m=1,2,3,\cdots$.

In the following, the first few terms of the coefficients $\mathscr{C}_i(x)$, $i=1,2,\cdots,m$, of expression (32) for each value of i will be calculated. To this end, the first series solution for $m=1$ takes the form

$$\upsilon_1(x,t)=20\kappa^2-30\kappa^2\tanh^2(\kappa x)+\frac{1}{\alpha}\mathscr{C}_1(x)t^\alpha, \tag{35}$$

while the first residual function takes the form

$$\mathscr{R}_s^1(x,t)=\frac{\partial^\alpha \upsilon_1}{\partial t}+2\upsilon_1^2\frac{\partial \upsilon_1}{\partial x}+6\frac{\partial \upsilon_1}{\partial x}\frac{\partial^2 \upsilon_1}{\partial x^2}+3\upsilon_1\frac{\partial^3 \upsilon_1}{\partial x^3}+\frac{\partial^5 \upsilon_1}{\partial x^5}. \tag{36}$$

Consequently, putting $\upsilon_1(x,t)$ into $\mathscr{R}_s^1(x,t)$ to get

$$\begin{aligned}\mathscr{R}_s^1(x,t)&=\mathscr{C}_1(x)\\&+2\left(\mathscr{C}_0(x)+\mathscr{C}_1(x)\frac{t^\alpha}{\alpha}\right)^2\left(\mathscr{C}_0'(x)+\mathscr{C}_1'(x)\frac{t^\alpha}{\alpha}\right)\\&+6\left(\mathscr{C}_0'(x)+\mathscr{C}_1'(x)\frac{t^\alpha}{\alpha}\right)\left(\mathscr{C}_0''(x)+\mathscr{C}_1''(x)\frac{t^\alpha}{\alpha}\right)\\&+3\left(\mathscr{C}_0(x)+\mathscr{C}_1(x)\frac{t^\alpha}{\alpha}\right)\left(\mathscr{C}_0^{(3)}(x)+\mathscr{C}_1^{(3)}(x)\frac{t^\alpha}{\alpha}\right)\\&+\left(\mathscr{C}_0^{(5)}(x)+\mathscr{C}_1^{(5)}(x)\frac{t^\alpha}{\alpha}\right).\end{aligned} \tag{37}$$

Thus, with the aid of $\mathscr{R}_s^1(x,t)_{|t=0}=0$, it yields

$$\mathscr{C}_1(x)+2\mathscr{C}_0'(x)\left(3\mathscr{C}_0''(x)+\mathscr{C}_0^2(x)\right)+3\mathscr{C}_0(x)\mathscr{C}_0^{(3)}(x)+\mathscr{C}_0^{(5)}(x)=0, \tag{38}$$

which implies that

$$\mathscr{C}_1(x)=5760\kappa^7\text{sech}^2(\kappa x)\tanh(\kappa x). \tag{39}$$

So, the first series solution $\upsilon_1(x,t)$ is provided by

$$\upsilon_1(x,t)=20\kappa^2-30\kappa^2\tanh^2(\kappa x)+5760\kappa^7\text{sech}^2(\kappa x)\tanh(\kappa x)\frac{t^\alpha}{\alpha}. \tag{40}$$

Sequentially, calculate the second truncated series $\upsilon_2(x,t)$ of expression (32) by setting $m=2$ in the m th truncated residual error (20) so that

$$\mathscr{R}_s^2(x,t)=\frac{\partial^\alpha \upsilon_2}{\partial t}+2\upsilon_2^2\frac{\partial \upsilon_2}{\partial x}+6\frac{\partial \upsilon_2}{\partial x}\frac{\partial^2 \upsilon_2}{\partial x^2}+3\upsilon_2\frac{\partial^3 \upsilon_2}{\partial x^3}+\frac{\partial^5 \upsilon_2}{\partial x^5}, \tag{41}$$

where $\upsilon_2(x,t)$ takes the form as

$$\upsilon_2(x,t)=20\kappa^2-30\kappa^2\tanh^2(\kappa x)+5760\kappa^7\text{sech}^2(\kappa x)\tanh(\kappa x)\frac{t^\alpha}{\alpha}+\frac{1}{2\alpha^2}\mathscr{C}_2(x)t^{2\alpha}, \tag{42}$$

and then employing the differential operator $\partial^\alpha/\partial t$ on both sides of equation (41) to get

$$\frac{\partial^\alpha \mathscr{R}_s^2(x,t)}{\partial t} = \mathscr{C}_2(x) + \frac{\partial^\alpha}{\partial t}\left(2v_2^2\frac{\partial v_2}{\partial x} + 6\frac{\partial v_2}{\partial x}\frac{\partial^2 v_2}{\partial x^2} + 3v_2\frac{\partial^3 v_2}{\partial x^3}\right) + \mathscr{C}_1^{(5)}(x) + \mathscr{C}_2^{(5)}(x)\frac{t^\alpha}{\alpha}. \quad (43)$$

Solving the term $\partial^\alpha \mathscr{R}_s^2(x,t)/\partial t_{|t=0} = 0$ via Mathematica computing system leads to

$$\mathscr{C}_2(x) = 552960\kappa^{12}(-2 + \cosh(2\kappa x))\text{sech}^4(\kappa x). \quad (44)$$

So, the second series solution $v_2(x,t)$ is given by

$$v_2(x,t) = 20\kappa^2 - 30\kappa^2\tanh^2(\kappa x) + 5760\kappa^7\text{sech}^2(\kappa x)\tanh(\kappa x)\frac{t^\alpha}{\alpha} + 276480\kappa^{12}(-2+\cosh(2\kappa x))\text{sech}^4(\kappa x)\frac{t^{2\alpha}}{\alpha^2}. \quad (45)$$

Likewise, the third truncated series $v_3(x,t)$ of expression (32) can be calculated by setting $m = 3$ in the m th truncated residual error (34), operating $\partial^{2\alpha}/\partial t^2$ on both sides of the resulting relevant equation, and solving the term $\partial^{2\alpha}\mathscr{R}_s^3(x,t)/\partial t^2{}_{|t=0} = 0$ to get $\mathscr{C}_3(x)$ as follow

$$\mathscr{C}_3(x) = 53084160\kappa^{17}(\sinh(3\kappa x) - 11\sinh(\kappa x))\text{sech}^5(\kappa x), \quad (46)$$

which implies that the third series solution $v_3(x,t)$ takes the form

$$v_3(x,t) = 20\kappa^2 - 30\kappa^2\tanh^2(\kappa x) + 5760\kappa^7\text{sech}^2(\kappa x)\tanh(\kappa x)\frac{t^\alpha}{\alpha} + 276480\kappa^{12}(-2+\cosh(2\kappa x))\text{sech}^4(\kappa x)\frac{t^{2\alpha}}{\alpha^2} + 8847360\kappa^{17}(\sinh(3\kappa x) - 11\sinh(\kappa x))\text{sech}^5(\kappa x)\frac{t^{3\alpha}}{\alpha^3}. \quad (47)$$

Continuing likewise, the fourth series solution $v_4(x,t)$ takes the form

$$v_4(x,t) = 20\kappa^2 - 30\kappa^2\tanh^2(\kappa x) + 5760\kappa^7\text{sech}^2(\kappa x)\tanh(\kappa x)\frac{t^\alpha}{\alpha} + 276480\kappa^{12}(-2+\cosh(2\kappa x))\text{sech}^4(\kappa x)\frac{t^{2\alpha}}{\alpha^2} + 8847360\kappa^{17}(\sinh(3\kappa x) - 11\sinh(\kappa x))\text{sech}^5(\kappa x)\frac{t^{3\alpha}}{\alpha^3} + 212336640\kappa^{22}(33 - 26\cosh(2\kappa x) + \cosh(4\kappa x))\text{sech}^6(\kappa x)\frac{t^{4\alpha}}{\alpha^4}. \quad (48)$$

To end this process, it can be assumed that $v_4(x,t)$ is the approximate solution. Furthermore, the rest values of $\mathscr{C}_m(x)$ for each $m \geq 5$ can be computed similarly. Thereafter, by collecting the obtained terms in the pattern of an infinite series, the solution $v(x,t)$ of (29–30) can be entirely predicted. Particularly, the analytical solution for $\alpha = 1$ is given by the following expression

$$v(x,t) = 20\kappa^2 - 30\kappa^2\tanh^2(\kappa x) + 5760\kappa^7\text{sech}^2(\kappa x)\tanh(\kappa x)t + 276480\kappa^{12}(-2+\cosh(2\kappa x))\text{sech}^4(\kappa x)t^2 + 8847360\kappa^{17}(\sinh(3\kappa x) - 11\sinh(\kappa x))\text{sech}^5(\kappa x)t^3 + 212336640\kappa^{22}(33 - 26\cosh(2\kappa x) + \cosh(4\kappa x))\text{sech}^6(\kappa x)t^4 + \cdots, \quad (49)$$

which is the same solution obtained by q-HAM [23], BPM [24], and mADM [40], after some symbolic simplification of hyperbolic trigonometric identities, so that

$$v(x,t) = 20\kappa^2 - 30\kappa^2\tanh^2(\kappa(x - 96\kappa^4 t)). \quad (50)$$

In the following, some graphical results achieved by the presented algorithm for (29–30) are provided in Figs. 1 and 2. Three-dimensional surface plots of the exact solution and fourth approximate solution at $\alpha = 1$ are provided in Fig. 1 with $\kappa = 0.1$ over a large enough spatiotemporal domain $[-20, 20] \times [0, 6]$, which shows match the exact and approximate solutions. In Fig. 2, the motion and elevation of water wave surface of (29–30) are displayed in 2D plots based on the parametric values of κ such that $\kappa = 0.25$, 0.5, 0.75, and 1.25 at $t = 1$, $-20 \leq x \leq 20$, and $\alpha = 0.8$. The comparison of the achieved absolute errors $|v - v_3|$ for (29–30) are exhibited in Table 1 for different values of x and t when $\alpha = 1$ and $\kappa = 0.01$ that compared to the absolute errors obtained by the mADM [31]. The superiority and efficiency of the presented FCRPSA are obvious from these results.

4.2. Application 2: Time-fractional Sawada-Kotera equation

In this portion, consider the fractional Sawada-Kotera equation with time-FCD in the underlying model [23,24]:

$$\frac{\partial^\alpha v}{\partial t} + 45v^2\frac{\partial v}{\partial x} + 15\frac{\partial v}{\partial x}\frac{\partial^2 v}{\partial x^2} + 15v\frac{\partial^3 v}{\partial x^3} + \frac{\partial^5 v}{\partial x^5} = 0, \quad (51)$$

associated with the underlying initial condition

$$v(x,0) = 2\kappa^2\text{sech}^2(\kappa x), \quad (52)$$

where $0 < \alpha \leq 1$, κ is an arbitrary constant with $\kappa \neq 0$, $x \in [a,b]$, $t \geq 0$, and $v = v(x,t)$ is a sufficiently smooth function. This model is completely integrable, admits N-soliton solutions, and has an endless set of conservation laws. The fractional Sawada-Kotera equation is widely used in nonlinear physical phenomena, including capillary gravitational waves, soliton's theory, hydrodynamics, and electromagnetic [3-7].

Using the FCRPSA, the fractional truncated series solution $v_m(x,t)$ of (51–52) about $t = 0$ in view of (52) is given by

$$v_m(x,t) = 2\kappa^2\text{sech}^2(\kappa x) + \sum_{i=1}^{m}\mathscr{C}_i(x)\frac{t^{i\alpha}}{\alpha^i i!}, \quad (53)$$

and the residual error function $\mathscr{R}_s(x,t)$ is given by

$$\mathscr{R}_s(x,t) = \frac{\partial^\alpha v}{\partial t} + 45v^2\frac{\partial v}{\partial x} + 15\frac{\partial v}{\partial x}\frac{\partial^2 v}{\partial x^2} + 15v\frac{\partial^3 v}{\partial x^3} + \frac{\partial^5 v}{\partial x^5}. \quad (54)$$

In this direction as well, the m-term truncated residual $\mathscr{R}_s^m(x,t)$ of $\mathscr{R}_s(x,t)$ is given by

$$\mathscr{R}_s^m(x,t) = \frac{\partial^\alpha v_m}{\partial t} + 45v_m^2\frac{\partial v_m}{\partial x} + 15\frac{\partial v_m}{\partial x}\frac{\partial^2 v_m}{\partial x^2} + 15v_m\frac{\partial^3 v_m}{\partial x^3} + \frac{\partial^5 v_m}{\partial x^5}, \quad (55)$$

in which $\partial^{(m-1)\alpha}\mathscr{R}_s^m/\partial t_{|t=0} \equiv 0$ for each $m = 1, 2, 3, \cdots$.

In the following, the first few terms of the coefficients $\mathscr{C}_i(x)$, $i = 1, 2, 3, \cdots, m$, of expression (53) for each value of i will be calculated. To this end, the first series solution for $m = 1$ is

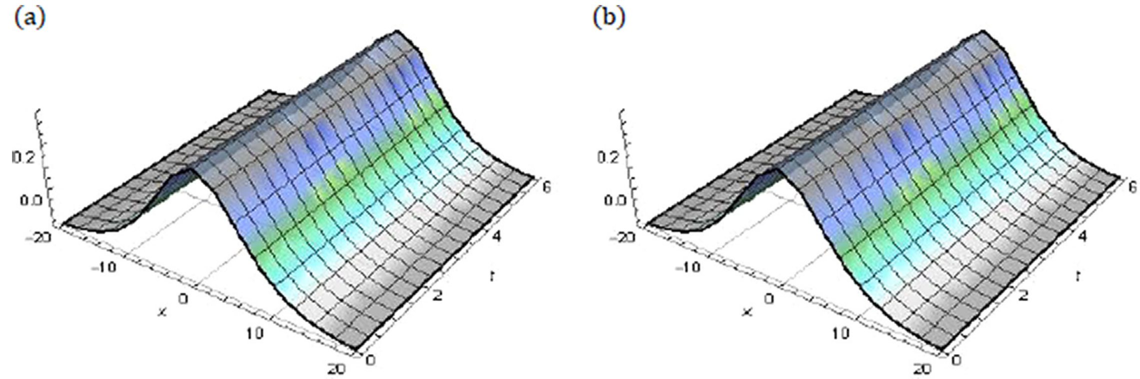

Fig. 1 Surface plots of time-fractional Ito model (29–30) with $\kappa = 0.1$ on $[-20, 20] \times [0, 6]$: (a) $v(x, t)$ and (b) $v_4(x, t)$ at $\alpha = 1$.

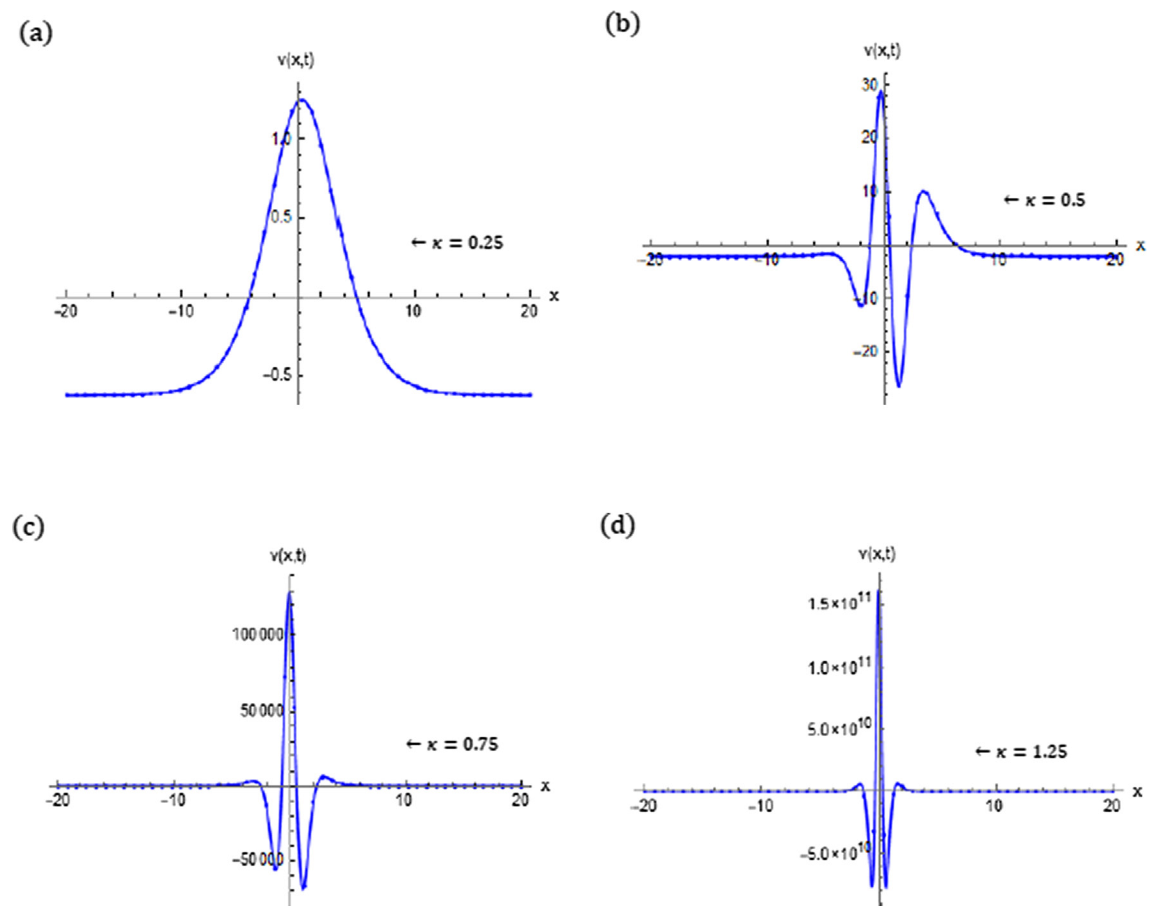

Fig. 2 Elevation of water wave surface of $v_4(x, t)$ of time-fractional Ito model (29–30) at $t = 1$ with fractional parameter $\alpha = 0.8$ and several parametric values of.κ.

$$v_1(x, t) = 2\kappa^2 \mathrm{sech}^2(\kappa x) + \frac{1}{\alpha}\mathscr{C}_1(x) t^{\alpha}, \tag{56}$$

and the first residual function is

$$\mathscr{R}^1_s(x, t) = \frac{\partial^{\alpha} v_1}{\partial t} + 45 v_1^2 \frac{\partial v_1}{\partial x} + 15 \frac{\partial v_1}{\partial x}\frac{\partial^2 v_1}{\partial x^2} + 15 v_1 \frac{\partial^3 v_1}{\partial x^3} + \frac{\partial^5 v_1}{\partial x^5}. \tag{57}$$

Consequently, putting $v_1(x, t)$ into $\mathscr{R}^1_s(x, t)$ to get

$$\begin{aligned}\mathscr{R}^1_s(x, t) = {} & \mathscr{C}_1(x) \\ & + 45\left(\mathscr{C}_0(x) + \mathscr{C}_1(x)\frac{t^{\alpha}}{\alpha}\right)^2 \left(\mathscr{C}_0'(x) + \mathscr{C}_1'(x)\frac{t^{\alpha}}{\alpha}\right) \\ & + 15\left(\mathscr{C}_0'(x) + \mathscr{C}_1'(x)\frac{t^{\alpha}}{\alpha}\right)\left(\mathscr{C}_0''(x) + \mathscr{C}_1''(x)\frac{t^{\alpha}}{\alpha}\right) \\ & + 15\left(\mathscr{C}_0(x) + \mathscr{C}_1(x)\frac{t^{\alpha}}{\alpha}\right)\left(\mathscr{C}_0^{(3)}(x) + \mathscr{C}_1^{(3)}(x)\frac{t^{\alpha}}{\alpha}\right) \\ & + \left(\mathscr{C}_0^{(5)}(x) + \mathscr{C}_1^{(5)}(x)\frac{t^{\alpha}}{\alpha}\right).\end{aligned} \tag{58}$$

Table 1 Comparison of absolute errors of time-fractional Ito model (29–30) with $\alpha = 1$ and $\kappa = 0.01$.

x_i	$t = 0.2$		$t = 0.6$		$t = 1.0$	
	FCRPSA	mADM [31]	FCRPSA	mADM [31]	FCRPSA	mADM [31]
2	2.7756×10^{-17}	1.4100×10^{-16}	0.0	1.4118×10^{-16}	2.7756×10^{-17}	1.4168×10^{-16}
4	3.8858×10^{-16}	5.6398×10^{-16}	3.6082×10^{-16}	5.6469×10^{-16}	3.3307×10^{-16}	5.6637×10^{-16}
6	4.1356×10^{-16}	1.2690×10^{-15}	4.0523×10^{-16}	1.2705×10^{-15}	3.9413×10^{-16}	1.2741×10^{-15}
8	1.0408×10^{-15}	2.2559×10^{-15}	9.9087×10^{-16}	2.2587×10^{-15}	8.9928×10^{-16}	2.2648×10^{-15}
10	2.3148×10^{-15}	3.5249×10^{-15}	2.2093×10^{-15}	3.5292×10^{-15}	2.0067×10^{-15}	3.5385×10^{-15}

Thus, with the aid of $\mathscr{R}^1_{\vartheta}(x,t)_{|t=0} = 0$, it yields

$$\mathscr{C}_1(x) + 15\Big(\mathscr{C}_0'(x)\Big(\mathscr{C}_0''(x) + 3\mathscr{C}_0^2(x)\Big) + \mathscr{C}_0(x)\mathscr{C}_0^{(3)}(x)\Big) + \mathscr{C}_0^{(5)}(x) = 0, \tag{59}$$

which implies that

$$\mathscr{C}_1(x) = 64\kappa^7 \tanh(\kappa x)\mathrm{sech}^2(\kappa x). \tag{60}$$

So, the first series solution $\upsilon_1(x,t)$ is provided by

$$\upsilon_1(x,t) = 2\kappa^2\mathrm{sech}^2(\kappa x) + 64\kappa^7 \tanh(\kappa x)\mathrm{sech}^2(\kappa x)\frac{t^\alpha}{\alpha}. \tag{61}$$

Sequentially, calculate the second truncated series $\upsilon_2(x,t)$ of expression (53) by setting $m = 2$ in the m th truncated residual error (55) so that

$$\mathscr{R}^2_{\vartheta}(x,t) = \frac{\partial^\alpha \upsilon_2}{\partial t} + 45\upsilon_2^2\frac{\partial \upsilon_2}{\partial x} + 15\frac{\partial \upsilon_2}{\partial x}\frac{\partial^2 \upsilon_2}{\partial x^2} + 15\upsilon_2\frac{\partial^3 \upsilon_2}{\partial x^3} + \frac{\partial^5 \upsilon_2}{\partial x^5}, \tag{62}$$

in which

$$\upsilon_2(x,t) = 2\kappa^2\mathrm{sech}^2(\kappa x) + 64\kappa^7 \tanh(\kappa x)\mathrm{sech}^2(\kappa x)\frac{t^\alpha}{\alpha} + \frac{1}{2\alpha^2}\mathscr{C}_2(x)t^{2\alpha}, \tag{63}$$

and employing the differential operator $\partial^\alpha/\partial t$ on both sides of the resulting equation (62) to get

$$\frac{\partial^\alpha \mathscr{R}^2_{\vartheta}(x,t)}{\partial t} = \mathscr{C}_2(x) + \frac{\partial^\alpha}{\partial t}\left(45\upsilon_2^2\frac{\partial \upsilon_2}{\partial x} + 15\frac{\partial \upsilon_2}{\partial x}\frac{\partial^2 \upsilon_2}{\partial x^2} + 15\upsilon_2\frac{\partial^3 \upsilon_2}{\partial x^3}\right) + \mathscr{C}_1^{(5)}(x) + \mathscr{C}_2^{(5)}(x)\frac{t^\alpha}{\alpha}. \tag{64}$$

Solving the term $\partial^\alpha\mathscr{R}^2_{\vartheta}(x,t)/\partial t_{|t=0} = 0$ via Mathematica computing system leads to

$$\mathscr{C}_2(x) = 1024\kappa^{12}(-2 + \cosh(2\kappa x))\mathrm{sech}^4(\kappa x). \tag{65}$$

So, the second series solution $\upsilon_2(x,t)$ is given by

$$\upsilon_2(x,t) = 2\kappa^2\mathrm{sech}^2(\kappa x) + 64\kappa^7 \tanh(\kappa x)\mathrm{sech}^2(\kappa x)\frac{t^\alpha}{\alpha} + 512\kappa^{12}(\cosh(2\kappa x) - 2)\mathrm{sech}^4(\kappa x)\frac{t^{2\alpha}}{\alpha^2}. \tag{66}$$

Likewise, the third truncated series $\upsilon_3(x,t)$ of expression (53) can be calculated by setting $m = 3$ in the m th truncated residual error (55), operating $\partial^{2\alpha}/\partial t^2$ on both sides of the resulting relevant equation, and solving the term $\partial^{2\alpha}\mathscr{R}^3_{\vartheta}(x,t)/\partial t^2{}_{|t=0} = 0$ to get $\mathscr{C}_3(x)$ as

$$\mathscr{C}_3(x) = 16384\kappa^{17}(\sinh(3\kappa x) - 11\sinh(\kappa x))\mathrm{sech}^5(\kappa x), \tag{67}$$

which implies that the third series solution $\upsilon_3(x,t)$ takes the form

$$\upsilon_3(x,t) = 2\kappa^2\mathrm{sech}^2(\kappa x) + 64\kappa^7 \tanh(\kappa x)\mathrm{sech}^2(\kappa x)\frac{t^\alpha}{\alpha} + 512\kappa^{12}(\cosh(2\kappa x) - 2)\mathrm{sech}^4(\kappa x)\frac{t^{2\alpha}}{\alpha^2} + \frac{8192}{3\alpha^3}\kappa^{17}(\sinh(3\kappa x) - 11\sinh(\kappa x))\mathrm{sech}^5(\kappa x)t^{3\alpha}. \tag{68}$$

Similarly, the fourth series solution $\upsilon_4(x,t)$ takes the form

$$\upsilon_4(x,t) = 2\kappa^2\mathrm{sech}^2(\kappa x) + 64\kappa^7 \tanh(\kappa x)\mathrm{sech}^2(\kappa x)\frac{t^\alpha}{\alpha} + 512\kappa^{12}(\cosh(2\kappa x) - 2)\mathrm{sech}^4(\kappa x)\frac{t^{2\alpha}}{\alpha^2} + \frac{8192}{3\alpha^3}\kappa^{17}(\sinh(3\kappa x) - 11\sinh(\kappa x))\mathrm{sech}^5(\kappa x)t^{3\alpha} + \frac{32768}{3\alpha^4}\kappa^{22}(33 - 26\cosh(2\kappa x) + \cosh(4\kappa x))\mathrm{sech}^6(\kappa x)t^{4\alpha}. \tag{69}$$

To end this process, it can be assumed that $\upsilon_4(x,t)$ is the approximate solution. Furthermore, the rest values of $\mathscr{C}_m(x)$ for each $m \geq 5$ can be computed similarly. Thereafter, by collecting the obtained terms in the pattern of an infinite series, the solution $\upsilon(x,t)$ of (51–52) can be entirely predicted. Particularly, the analytical solution for $\alpha = 1$ is given by the following expression

$$\upsilon(x,t) = 2\kappa^2\mathrm{sech}^2(\kappa x) + 64\kappa^7 \tanh(\kappa x)\mathrm{sech}^2(\kappa x)t + 512\kappa^{12}(\cosh(2\kappa x) - 2)\mathrm{sech}^4(\kappa x)t^2 + \frac{8192}{3\alpha^3}\kappa^{17}(\sinh(3\kappa x) - 11\sinh(\kappa x))\mathrm{sech}^5(\kappa x)t^3 + \frac{32768}{3\alpha^4}\kappa^{22}(33 - 26\cosh(2\kappa x) + \cosh(4\kappa x))\mathrm{sech}^6(\kappa x)t^4 + \cdots, \tag{70}$$

which meets the underlying exact solution provided by q-HAM [23] and BPM [24] through symbolic simplification of hyperbolic trigonometric identities

$$\upsilon(x,t) = 2\kappa^2\mathrm{sech}^2(\kappa(x - 16\kappa^4 t)). \tag{71}$$

Fig. 3 shows the three-dimensional plots of the exact solution and fourth approximate solution at $\alpha = 1$ for (51–52) when $\kappa = 0.3$ along with a large enough spatiotemporal domain $[-20, 20] \times [0, 10]$. Further, the motion and elevation of the water wave surface of (51–52) are displayed in 2D plots in Fig. 4 based on the time values of t such that $t \in \{0.2, 2, 4, 10\}$ with fractional parameter $\alpha = 0.9$ and $\kappa = 0.5$ on $-15 \le x \le 15$. The comparison of the achieved absolute errors $|v - v_2|$ for (51–52) are exhibited in Table 2 for different values of x and t when $\alpha = 1$ and $\kappa = 0.01$, which compared to the absolute errors obtained by BPM [24]. The efficiency of the presented FCRPSA is obvious from these results.

4.3. Application 3: Time-fractional Lax's Korteweg-de Vries equation

In this portion, consider the fractional Lax's KdV equation with time-FCD in the underlying model [5,40]:

$$\frac{\partial^\alpha v}{\partial t} + 30v^2\frac{\partial v}{\partial x} + 30\frac{\partial v}{\partial x}\frac{\partial^2 v}{\partial x^2} + 10v\frac{\partial^3 v}{\partial x^3} + \frac{\partial^5 v}{\partial x^5} = 0, \tag{72}$$

associated with the underlying initial condition

$$v(x,0) = 2\kappa^2(2 - 3\tanh^2(\kappa x)), \tag{73}$$

where $0 < \alpha \le 1$, κ is an arbitrary constant with $\kappa \neq 0$, $x \in [a, b]$, $t \ge 0$, and $v = v(x,t)$ is a sufficiently smooth function. Such an equation is completely integrable, admits N-soliton solutions, and has an endless set of conservation laws [14]. The exact solution of (72–73) is given by [5,41]

$$v(x,t) = 2\kappa^2\left(2 - 3\tanh^2\left(\kappa(x - 56\kappa^4 t)\right)\right). \tag{74}$$

Using the FCRPSA, the fractional truncated series solution $v_m(x,t)$ of (72–73) about $t = 0$ in view of (73) takes the form

$$v_m(x,t) = 2\kappa^2(2 - 3\tanh^2(\kappa x)) + \sum_{i=1}^{m} \mathscr{C}_i(x)\frac{t^{i\alpha}}{\alpha^i i!}, \tag{75}$$

provided that $\mathscr{C}_0(x) = v(x,0)$.

In this orientation as well, the m-term residual function $\mathscr{R}_s^m(x,t)$ is given by

$$\mathscr{R}_s^m(x,t) = \frac{\partial^\alpha v_m}{\partial t} + 30v_m^2\frac{\partial v_m}{\partial x} + 30\frac{\partial v_m}{\partial x}\frac{\partial^2 v_m}{\partial x^2} + 10v_m\frac{\partial^3 v_m}{\partial x^3} + \frac{\partial^5 v_m}{\partial x^5}, \tag{76}$$

in which $\partial^{(m-1)\alpha}\mathscr{R}_s^m/\partial t_{|t=0} \equiv 0$ for each $m = 1, 2, 3, \cdots$.

Now, the first series solution for $m = 1$ takes the form

$$v_1(x,t) = 2\kappa^2(2 - 3\tanh^2(\kappa x)) + \frac{1}{\alpha}\mathscr{C}_1(x)t^\alpha, \tag{77}$$

while the first residual function takes the form

$$\mathscr{R}_s^1(x,t) = \frac{\partial^\alpha v_1}{\partial t} + 30v_1^2\frac{\partial v_1}{\partial x} + 30\frac{\partial v_1}{\partial x}\frac{\partial^2 v_1}{\partial x^2} + 10v_1\frac{\partial^3 v_1}{\partial x^3} + \frac{\partial^5 v_1}{\partial x^5}. \tag{1}$$

Consequently, putting $v_1(x,t)$ into $\mathscr{R}_s^1(x,t)$, and using the term $\mathscr{R}_s^1(x,t)_{|t=0} = 0$ to get

$$\mathscr{C}_1(x) + 30\mathscr{C}_0'(x)\left(\mathscr{C}_0''(x) + \mathscr{C}_0^2(x)\right) + 10\mathscr{C}_0(x)\mathscr{C}_0^{(3)}(x) + \mathscr{C}_0^{(5)}(x) = 0, \tag{78}$$

which implies that

$$\mathscr{C}_1(x) = 672\kappa^7\left(\tanh(\kappa x) - \tanh^3(\kappa x)\right). \tag{79}$$

In this case, the first series solution $v_1(x,t)$ is given by

$$v_1(x,t) = 2\kappa^2(2 - 3\tanh^2(\kappa x)) + 672\kappa^7\left(\tanh(\kappa x) - \tanh^3(\kappa x)\right)\frac{t^\alpha}{\alpha}. \tag{80}$$

Sequentially, by setting $m = 2$ in the m th truncated residual error (76), applying $\partial^\alpha/\partial t$ on both sides of the resulting relevant equation, and solving the term $\partial^\alpha\mathscr{R}_s^2(x,t)/\partial t_{|t=0} = 0$, the second series solution $v_2(x,t)$ can be obtained as

$$v_2(x,t) = 2\kappa^2(2 - 3\tanh^2(\kappa x)) + 672\kappa^7 \times \tanh(\kappa x)\operatorname{sech}^2(\kappa x)\frac{t^\alpha}{\alpha} + 18816\kappa^{12}(\cosh(2\kappa x) - 2)\operatorname{sech}^4(\kappa x)\frac{t^{2\alpha}}{\alpha^2}. \tag{81}$$

Likewise, by setting $m = 3$ in the m th truncated residual error (76), operating $\partial^{2\alpha}/\partial t^2$ on both sides of the resulting relevant equation, and solving the term $\partial^{2\alpha}\mathscr{R}_s^3(x,t)/\partial t^2{}_{|t=0} = 0$, the third series solution $v_3(x,t)$ can be obtained as

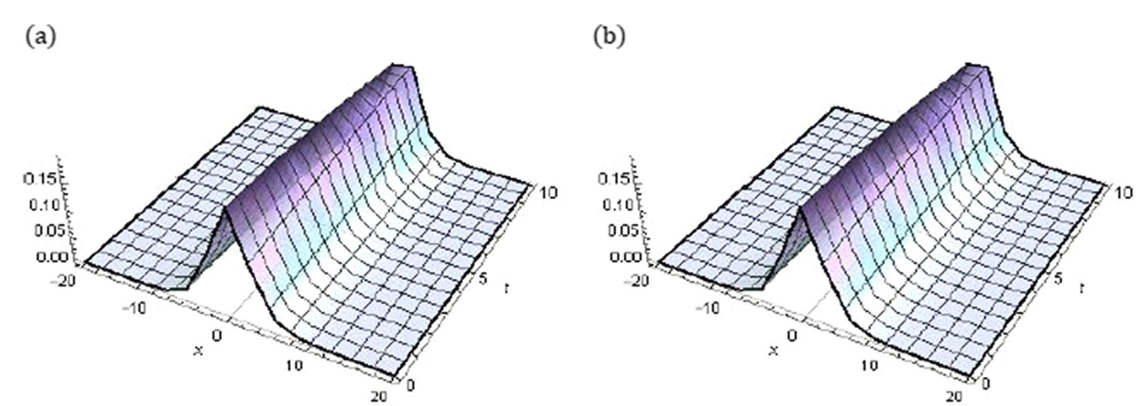

Fig. 3 Surface plots of time-fractional Sawada-Kotera model (51–52) with $\kappa = 0.3$, $(x,t) \in [-20, 20] \times [0, 10]$: (a) $v(x,t)$ and (b) $v_4(x,t)$ at $\alpha = 1$.

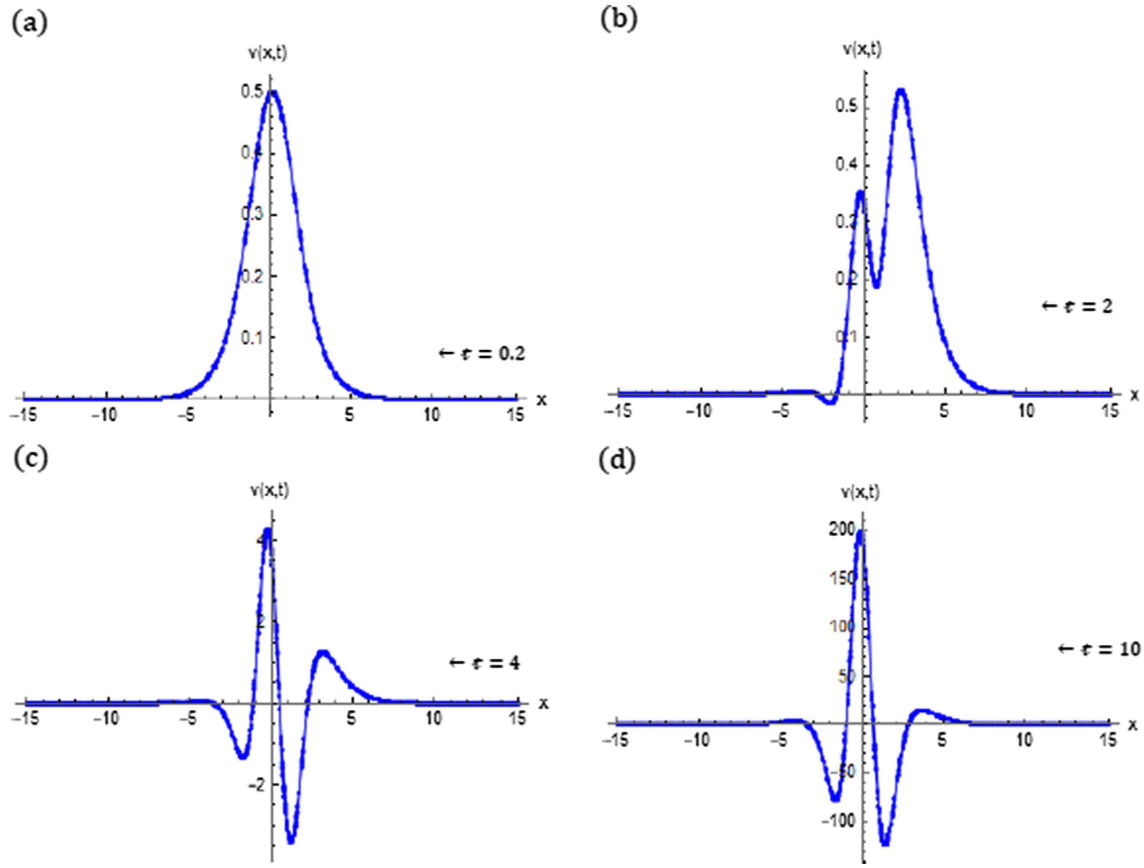

Fig. 4 Elevation of water wave surface of $v_4(x,t)$ of time-fractional Sawada-Kotera model (51–52) with fractional parameter $\alpha = 0.9$ and $\kappa = 0.5$, and different time values t.

Table 2 Comparison of absolute errors of time-fractional Sawada-Kotera model (51–52) at $\alpha = 1$.

x_i	$t = 0.1$		$t = 0.5$		$t = 0.9$	
	$\lvert v - v_2\rvert$	BPM [24]	$\lvert v - v_2\rvert$	BPM [24]	$\lvert v - v_2\rvert$	BPM [24]
2	3.4695×10^{-18}	2.79×10^{-12}	2.7062×10^{-16}	1.81×10^{-12}	1.5960×10^{-15}	1.86×10^{-11}
4	3.4695×10^{-18}	1.44×10^{-12}	8.2226×10^{-16}	6.56×10^{-13}	4.7566×10^{-15}	1.06×10^{-11}
6	1.0408×10^{-17}	9.88×10^{-14}	1.3531×10^{-15}	4.94×10^{-13}	7.9034×10^{-15}	2.67×10^{-12}
8	1.3878×10^{-17}	1.25×10^{-12}	1.8804×10^{-15}	1.64×10^{-12}	1.0984×10^{-14}	5.30×10^{-12}
10	1.7347×10^{-17}	2.59×10^{-12}	2.3974×10^{-15}	2.79×10^{-12}	1.4003×10^{-14}	1.33×10^{-11}

$$\begin{aligned} v_3(x,t) &= 2\kappa^2(2 - 3\tanh^2(\kappa x)) + 672\kappa^7 \\ &\quad \times \tanh(\kappa x)\operatorname{sech}^2(\kappa x)\frac{t^\alpha}{\alpha} \\ &\quad + 18816\kappa^{12}(\cosh(2\kappa x) - 2)\operatorname{sech}^4(\kappa x)\frac{t^{2\alpha}}{\alpha^2} \\ &\quad + 351232\kappa^{17}(\sinh(3\kappa x) - 11\sinh(\kappa x))\operatorname{sech}^5(\kappa x)\frac{t^{3\alpha}}{\alpha^3}. \end{aligned} \tag{82}$$

Similarly, the rest of $\mathscr{C}_m(x)$ for each $m \geq 4$ can be computed. Thereafter, by collecting the obtained terms in the pattern of an infinite series, the solution $v(x,t)$ of (72–73) can be entirely predicted. The solution (82) for $\alpha = 1$ is fully compatible with the solution achieved by mADM [40] and mVIM [41].

In the following, the 2D plots of fractional level curves for (72–73) are displayed in Fig. 5 based on different fractional indices such that $\alpha \in \{0.25, 0.5, 0.75, 1.0\}$ with $\kappa = 0.3$ and $\kappa = 0.35$ for $t = 4$ and $-10 \leq x \leq 10$. The comparison of the achieved absolute errors $\lvert v - v_3\rvert$ for (72–73) are reported in Table 3 for different values of x and t when $\alpha = 1$ and $\kappa = 0.01$, which compared to the absolute errors obtained by the mADM [40] and mVIM [41]. The superiority and efficiency of the presented FCRPSA are obvious from these results.

4.4. Application 4: Time-fractional Caudrey-Dodd-Gibbon equation

In this portion, consider the fractional Caudrey-Dodd-Gibbon equation with time-FCD in the underlying model [40,41]:

$$\frac{\partial^\alpha v}{\partial t}+180v^2\frac{\partial v}{\partial x}+30\frac{\partial v}{\partial x}\frac{\partial^2 v}{\partial x^2}+30v\frac{\partial^3 v}{\partial x^3}+\frac{\partial^5 v}{\partial x^5}=0, \tag{83}$$

associated with the underlying initial condition

$$v(x,0)=\frac{\kappa e^{\kappa x}}{(1+e^{\kappa x})^2}, \tag{84}$$

where $0<\alpha\leq 1$, κ is an arbitrary constant with $\kappa\neq 0$, $x\in[a,b]$, $t\geq 0$, and v is a sufficiently smooth function.

Using the FCRPSA, the fractional truncated series solution $v_m(x,t)$ of (83–84) about $t=0$ in view of (84) takes the form

$$v_m(x,t)=\frac{\kappa e^{\kappa x}}{(1+e^{\kappa x})^2}+\sum_{i=1}^{m}\mathcal{C}_i(x)\frac{t^{i\alpha}}{\alpha^i i!}, \tag{85}$$

while the m-term residual function $\mathcal{R}_s^m(x,t)$ takes the form

$$\mathcal{R}_s^m(x,t)=\frac{\partial^\alpha v_m}{\partial t}+180v_m^2\frac{\partial v_m}{\partial x}+30\frac{\partial v_m}{\partial x}\frac{\partial^2 v_m}{\partial x^2}+30v_m\times\frac{\partial^3 v_m}{\partial x^3}+\frac{\partial^5 v_m}{\partial x^5}. \tag{86}$$

Consequently, the first series solution for $m=1$ is given by

$$v_1(x,t)=\kappa e^{\kappa x}(1+e^{\kappa x})^{-2}+\frac{1}{\alpha}\mathcal{C}_1(x)t^\alpha, \tag{87}$$

and the first residual function is given by

$$\mathcal{R}_s^1(x,t)=\frac{\partial^\alpha v_1}{\partial t}+180v_m^2\frac{\partial v_m}{\partial x}+30\frac{\partial v_1}{\partial x}\frac{\partial^2 v_1}{\partial x^2}+30v_1\frac{\partial^3 v_1}{\partial x^3}+\frac{\partial^5 v_1}{\partial x^5}. \tag{88}$$

Putting $v_1(x,t)$ into $\mathcal{R}_s^1(x,t)$, and using the term $\mathcal{R}_s^1(x,t)_{|t=0}=0$ to get

$$\mathcal{C}_1(x)+30\left(\mathcal{C}_0'(x)\left(\mathcal{C}_0''(x)+6\mathcal{C}_0^2(x)\right)+\mathcal{C}_0(x)\mathcal{C}_0^{(3)}(x)\right)+\mathcal{C}_0^{(5)}(x)=0, \tag{89}$$

which implies that

$$\mathcal{C}_1(x)=\frac{\kappa^7 e^{\kappa x}(e^{\kappa x}-1)}{(1+e^{\kappa x})^3}. \tag{90}$$

Thus, the first series solution $v_1(x,t)$ is given as

$$v_1(x,t)=\frac{\kappa e^{\kappa x}}{(1+e^{\kappa x})^2}+\frac{\kappa^7 e^{\kappa x}(e^{\kappa x}-1)}{\alpha(1+e^{\kappa x})^3}t^\alpha. \tag{91}$$

Sequentially, by setting $m=2$ in the m th truncated residual error (86), applying $\partial^\alpha/\partial t$ on both sides of the resulting equation, and solving $\partial^\alpha\mathcal{R}_s^2(x,t)/\partial t_{|t=0}=0$, we get the second series solution $v_2(x,t)$ as

$$v_2(x,t)=\frac{\kappa e^{\kappa x}}{(1+e^{\kappa x})^2}+\frac{\kappa^7 e^{\kappa x}(e^{\kappa x}-1)}{\alpha(1+e^{\kappa x})^3}t^\alpha+\frac{\kappa^{12}e^{\kappa x}(1-4e^{\kappa x}+e^{2\kappa x})}{2\alpha^2(1+e^{\kappa x})^4}t^{2\alpha}. \tag{92}$$

Likewise, by setting $m=3$ in the m th truncated residual error (86), operating $\partial^{2\alpha}/\partial t^2$ on both sides of the resulting relevant equation, and solving the term $\partial^{2\alpha}\mathcal{R}_s^3(x,t)/\partial t^2{}_{|t=0}=0$, we get the third series solution $v_3(x,t)$ as

$$v_3(x,t)=\frac{\kappa e^{\kappa x}}{(1+e^{\kappa x})^2}+\frac{\kappa^7 e^{\kappa x}(e^{\kappa x}-1)}{\alpha(1+e^{\kappa x})^3}t^\alpha+\frac{\kappa^{12}e^{\kappa x}(1-4e^{\kappa x}+e^{2\kappa x})}{2\alpha^2(1+e^{\kappa x})^4}t^{2\alpha}+\frac{\kappa^{17}e^{\kappa x}(e^{\kappa x}-1)(1-10e^{\kappa x}+e^{2\kappa x})}{6(1+e^{\kappa x})^5}t^{3\alpha}. \tag{93}$$

Similarly, the fourth series solution $v_4(x,t)$ takes the form

$$v_4(x,t)=\frac{\kappa e^{\kappa x}}{(1+e^{\kappa x})^2}+\frac{\kappa^7 e^{\kappa x}(e^{\kappa x}-1)}{\alpha(1+e^{\kappa x})^3}t^\alpha+\frac{\kappa^{12}e^{\kappa x}(1-4e^{\kappa x}+e^{2\kappa x})}{2\alpha^2(1+e^{\kappa x})^4}t^{2\alpha}+\frac{\kappa^{17}e^{\kappa x}(e^{\kappa x}-1)(1-10e^{\kappa x}+e^{2\kappa x})}{6\alpha^3(1+e^{\kappa x})^5}t^{3\alpha}+\frac{\kappa^{22}e^{\kappa x}(1-26e^{\kappa x}+66e^{2\kappa x}-26e^{3\kappa x}+e^{4\kappa x})}{24\alpha^4(1+e^{\kappa x})^6}t^{4\alpha}. \tag{94}$$

To end this process, it can be assumed that $v_4(x,t)$ is the approximate solution. Nevertheless, the rest values of $\mathcal{C}_m(x)$ for each $m\geq 5$ can be computed similarly. Thereafter, by collecting the obtained terms in the pattern of an infinite series,

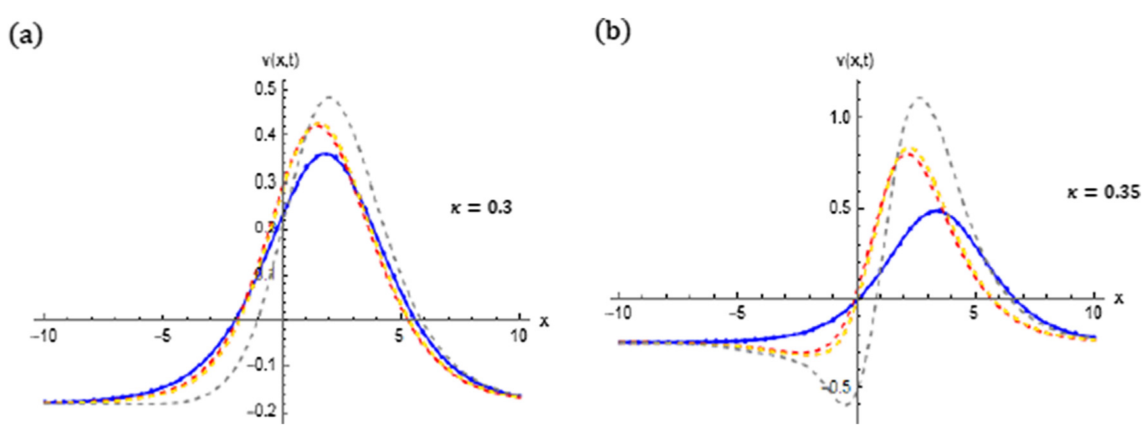

Fig. 5 Elevation of water surface of the wavefunction $v_3(x,t)$ for fractional Lax's KdV model (72–73) at $t=4$ with different fractional-index values: $\alpha=1$ blue, $\alpha=0.75$ red, $\alpha=0.5$ yellow and $\alpha=0.25$ gray.

Table 3 Comparison of absolute errors of fractional Lax's KdV model (72–73) with $\alpha = 1$ and $\kappa = 0.01$.

x_i	$t = 0.8$			$t = 5$		
	FCRPSA	mVIA [32]	mADM [31]	FCRPSA	mVIA [32]	mADM [31]
2	1.3444×10^{-17}	2.2991×10^{-13}	2.3034×10^{-13}	5.1738×10^{-16}	1.4369×10^{-12}	1.4210×10^{-12}
4	1.3010×10^{-17}	4.5688×10^{-13}	4.6073×10^{-13}	5.0871×10^{-16}	2.8555×10^{-12}	2.8421×10^{-12}
6	1.2794×10^{-17}	6.7804×10^{-13}	6.1915×10^{-13}	4.9418×10^{-16}	4.2377×10^{-12}	4.2633×10^{-12}
8	1.2143×10^{-17}	8.9060×10^{-13}	9.2162×10^{-13}	4.7380×10^{-16}	5.5662×10^{-12}	5.6844×10^{-12}
10	1.1493×10^{-17}	1.0919×10^{-13}	1.1521×10^{-12}	4.4929×10^{-16}	6.8246×10^{-12}	7.1057×10^{-12}

the solution $v(x,t)$ of (83–84) can be entirely predicted. Particularly, the analytical solution for $\alpha = 1$ is given by the following expression

$$v(x,t) = \frac{\kappa e^{\kappa x}}{(1+e^{\kappa x})^2} + \frac{\kappa^7 e^{\kappa x}(e^{\kappa x}-1)}{(1+e^{\kappa x})^3}t + \frac{\kappa^{12} e^{\kappa x}(1-4e^{\kappa x}+e^{2\kappa x})}{2(1+e^{\kappa x})^4}t^2 + \frac{\kappa^{17} e^{\kappa x}(e^{\kappa x}-1)(1-10e^{\kappa x}+e^{2\kappa x})}{6(1+e^{\kappa x})^5}t^3 + \frac{\kappa^{22} e^{\kappa x}(1-26e^{\kappa x}+66e^{2\kappa x}-26e^{3\kappa x}+e^{4\kappa x})}{24(1+e^{\kappa x})^6}t^4 + \cdots, \tag{95}$$

which meets the underlying exact solution provided by mADM [40] after some symbolic simplification of hyperbolic trigonometric identities

$$v(x,t) = \kappa e^{\kappa(x-\kappa^4 t)}\left(1+e^{\kappa(x-\kappa^4 t)}\right)^{-2}. \tag{96}$$

In the following, the 3D plots of absolute error $|v - v_3|$ for (83–84) with $\kappa = 0.3$ are plotted in Fig. 6 for fractional orders $\alpha = 1$ and $\alpha = 0.75$ over a large enough spatiotemporal domain $[-20, 20] \times [0, 4]$. The comparison of the achieved absolute errors $|v - v_3|$ for (83–84) are reported in Table 4 for different values of x and t when $\alpha = 1$ and $\kappa = 0.01$, which compared to the absolute errors obtained by mVIM [41] and mADM [40]. The accuracy and efficiency of the presented FCRPSA are obvious from these results.

4.5. Application 5 Time-fractional Kaup-Kupershmidt equation

In this portion, consider the fractional Kaup-Kupershmidt equation with time-FCD in the underlying model [42]:

$$\frac{\partial^\alpha v}{\partial t} + 45v^2\frac{\partial v}{\partial x} - 15\rho\frac{\partial v}{\partial x}\frac{\partial^2 v}{\partial x^2} - 15v\frac{\partial^3 v}{\partial x^3} + \frac{\partial^5 v}{\partial x^5} = 0, 0 < \alpha \le 1, \tag{97}$$

associated with the underlying initial condition

$$v(x,0) = \frac{1}{4}\omega^2\lambda^2\text{sech}^2\left(\frac{\lambda\omega x}{2}\right) + \frac{1}{12}\omega^2\lambda^2, \tag{98}$$

where $x \in [a,b]$, $t \ge 0$, v is a sufficiently differentiable function. This equation is integrable for $\rho = 5/2$. The exact solution of (97–98) is provided in [42] as follows

$$v(x,t) = \frac{1}{4}\omega^2\lambda^2\text{sech}^2\left(\frac{\lambda}{2}\left(\frac{\xi}{\alpha}t^\alpha + \omega x\right)\right) + \frac{1}{12}\omega^2\lambda^2, \tag{99}$$

where $\xi = \frac{-\omega^5}{16}\left(-8\lambda^2\mu + 16\mu^2 + \lambda^4\right)$, ω, λ, and μ are arbitrary real parameters with $\omega \neq 0$.

Using the FCRPSA, the fractional truncated series solution $v_m(x,t)$ of (97–98) about $t = 0$ in view of (98) is given as follows:

$$v_m(x,t) = \frac{1}{4}\omega^2\lambda^2\text{sech}^2\left(\frac{\lambda\omega x}{2}\right) + \frac{1}{12}\omega^2\lambda^2 + \sum_{i=1}^{m}\mathscr{C}_i(x)\frac{t^{i\alpha}}{\alpha^i i!}. \tag{100}$$

In this orientation as well, the m-term residual function $\mathscr{R}_s^m(x,t)$ is given by

$$\mathscr{R}_s^m(x,t) = \frac{\partial^\alpha v_m}{\partial t} + 45v_m^2\frac{\partial v_m}{\partial x} - 15\rho\frac{\partial v_m}{\partial x}\frac{\partial^2 v_m}{\partial x^2} - 15v_m \times \frac{\partial^3 v_m}{\partial x^3} + \frac{\partial^5 v_m}{\partial x^5}, \tag{101}$$

in which $\partial^{(m-1)\alpha}\mathscr{R}_s^m/\partial t_{|t=0} \equiv 0$ for each $m = 1, 2, 3, \cdots$.

In the following, the first few terms of the coefficients $\mathscr{C}_i(x)$, $i = 1, 2, 3, \cdots, m$, of expression (100) for each value of i will be calculated. To this end, the first series solution for $m = 1$ takes the form

$$v_1(x,t) = \frac{1}{4}\omega^2\lambda^2\text{sech}^2\left(\frac{\lambda\omega x}{2}\right) + \frac{1}{12}\omega^2\lambda^2 + \frac{1}{\alpha}\mathscr{C}_1(x)t^\alpha, \tag{102}$$

and the first residual function takes the form

$$\mathscr{R}_s^1(x,t) = \frac{\partial^\alpha v_1}{\partial t} + 45v_1^2\frac{\partial v_1}{\partial x} - 15\rho\frac{\partial v_1}{\partial x}\frac{\partial^2 v_1}{\partial x^2} - 15v_1 \times \frac{\partial^3 v_1}{\partial x^3} + \frac{\partial^5 v_1}{\partial x^5}. \tag{103}$$

Consequently, putting $v_1(x,t)$ into $\mathscr{R}_s^1(x,t)$, and using $\mathscr{R}_s^1(x,t)_{|t=0} = 0$ to get

$$\mathscr{C}_1(x) - 15\left(\mathscr{C}_0'(x)\left(\rho\mathscr{C}_0''(x) - 3\mathscr{C}_0^2(x)\right) + \mathscr{C}_0(x)\mathscr{C}_0^{(3)}(x)\right) + \mathscr{C}_0^{(5)}(x) = 0, \tag{104}$$

which implies that

$$\mathscr{C}_1(x) = \frac{1}{512}\omega^7\lambda^7(3843 + 480p - 4(209 + 60\rho)\cosh(wx\lambda) + \cosh(2wx\lambda))\tanh(\frac{wx\lambda}{2})\text{sech}^6(\frac{wx\lambda}{2}). \tag{105}$$

Thus, the first series solution $v_1(x,t)$ is given by

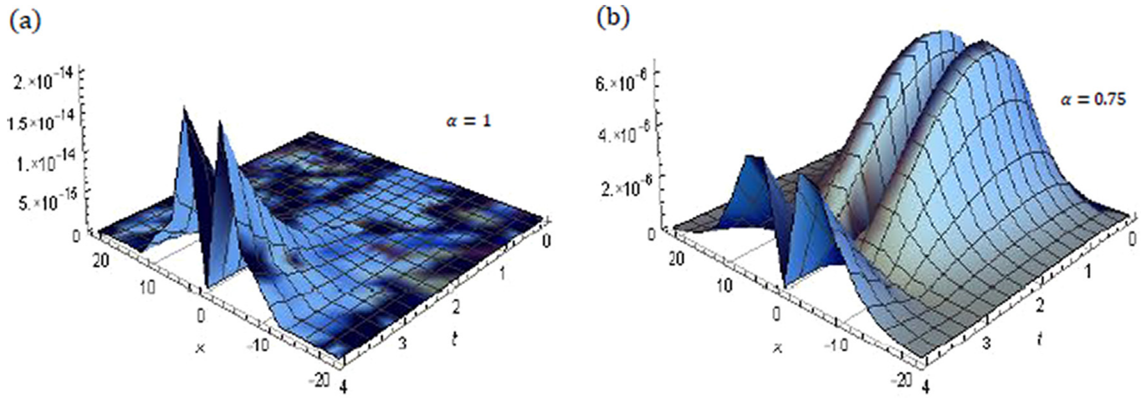

Fig. 6 3D plots of $|\upsilon - \upsilon_3|$ for fractional Caudrey-Dodd-Gibbon model (83–84) with $\kappa = 0.3$.

Table 4 Comparison of absolute error of fractional Caudrey-Dodd-Gibbon model (83–84) at $\alpha = 1$ and $\kappa = 0.01$.

x_i	$t = 0.8$			$t = 5$		
	FCRPSA	mVIA [32]	mADM [31]	FCRPSA	mVIA [32]	mADM [31]
2	0	6.7763×10^{-21}	1.7893×10^{-20}	1.0164×10^{-21}	3.3881×10^{-21}	2.4803×10^{-18}
4	1.3553×10^{-20}	1.0164×10^{-20}	2.0134×10^{-20}	0	1.3553×10^{-20}	5.7068×10^{-18}
6	3.3881×10^{-21}	3.3881×10^{-21}	3.9146×10^{-20}	3.3881×10^{-21}	6.7763×10^{-21}	8.9310×10^{-18}
8	6.7763×10^{-21}	0	5.7990×10^{-20}	6.7763×10^{-20}	1.3553×10^{-20}	1.2180×10^{-17}
10	0	3.3881×10^{-21}	5.6336×10^{-20}	3.3881×10^{-21}	0	1.5409×10^{-17}

$$\begin{aligned}\upsilon_1(x,t) = {} & \frac{1}{12}\omega^2\lambda^2 + \frac{1}{4}\omega^2\lambda^2\text{sech}^2\left(\frac{\lambda\omega x}{2}\right) \\ & + \frac{1}{512}\omega^7\lambda^7(3843 + 480\rho - 4(209 \\ & + 60\rho)\cosh(\lambda\omega x) \\ & + \cosh(2\lambda\omega x))\tanh\left(\frac{\lambda\omega x}{2}\right)\text{sech}^6\left(\frac{\lambda\omega x}{2}\right)\frac{t^\alpha}{\alpha}.\end{aligned} \tag{106}$$

Sequentially, by setting $m = 2$ in the m th truncated residual error (101), applying $\partial^\alpha/\partial t$ on both sides of the resulting equation, and solving $\partial^\alpha \mathcal{R}_\upsilon^2(x,t)/\partial t_{|t=0} = 0$, we get the second solution $\upsilon_2(x,t)$ as follows:

$$\begin{aligned}\upsilon_2(x,t) = {} & \frac{1}{12}\omega^2\lambda^2 + \frac{1}{4}\omega^2\lambda^2\text{sech}^2\left(\frac{\lambda\omega x}{2}\right) \\ & + \frac{1}{512}\omega^7\lambda^7(3843 + 480\rho - 4(209 + 60\rho)\cosh(\lambda\omega x) \\ & + \cosh(2\lambda\omega x))\tanh\left(\frac{\lambda\omega x}{2}\right)\text{sech}^6\left(\frac{\lambda\omega x}{2}\right)\frac{t^\alpha}{\alpha} \\ & + \frac{1}{1048576}\omega^{12}\lambda^{12}(\zeta_1 + \zeta_2\cosh(\lambda\omega x) - \zeta_3\cosh(2\lambda\omega x) \\ & + 3\zeta_4\cosh(3\lambda\omega x) - \zeta_5\cosh(4\lambda\omega x) \\ & + \cosh(5\lambda\omega x))\text{sech}^{12}\left(\frac{\lambda\omega x}{2}\right)\frac{t^{2\alpha}}{\alpha^2},\end{aligned} \tag{107}$$

in which

$$\begin{aligned}\zeta_1 &= -12(328935727 + 240\rho(254677 + 7200\rho)), \\ \zeta_2 &= 6(777305099 + 640\rho(231379 + 6810\rho)), \\ \zeta_3 &= 48(18859301 + 40\rho(96263 + 3120\rho)), \\ \zeta_4 &= 15437759 + 3840\rho(893 + 30\rho), \\ \zeta_5 &= 4(76439 + 21840\rho).\end{aligned} \tag{108}$$

Likewise, the third truncated series $\upsilon_3(x,t)$ of expression (100) can be calculated by setting $m = 3$ in the m th truncated residual error (101), operating $\partial^{2\alpha}/\partial t^2$ on both sides of the resulting relevant equation, and solving the term $\partial^{2\alpha}\mathcal{R}_\upsilon^3(x,t)/\partial t^2{}_{|t=0} = 0$. To end this process, it can be assumed that $\upsilon_3(x,t)$ is the approximate solution. The rest values of $\mathcal{C}_m(x)$ for each $m \geq 4$ can be computed similarly. Thereafter, by collecting the obtained terms in the pattern of an infinite series, the solution $\upsilon(x,t)$ of (97–98) can be entirely predicted.

In the following, the surface and contour plots of the third approximate solution for (97–98) are displayed in Fig. 7 with $\lambda = 0.1$, $\mu = 0$, $\omega = 1$, and $\alpha = 0.75$ over a large enough spatiotemporal domain $[-40, 40] \times [0, 10]$. The comparison of the achieved absolute errors $|\upsilon - \upsilon_2|$ for (97–98) are summarized in Table 5 for different values of x and t when $\alpha = 1$, which compared to the absolute errors obtained by LMM and OHAM [42]. The accuracy and efficiency of the FCRPSA are obvious from these results.

5. Discussions and concluding remarks

This paper adopted the FCRPSA to solve a class of the time-FNEEs in terms of FCD sense, including time-fractional Ito,

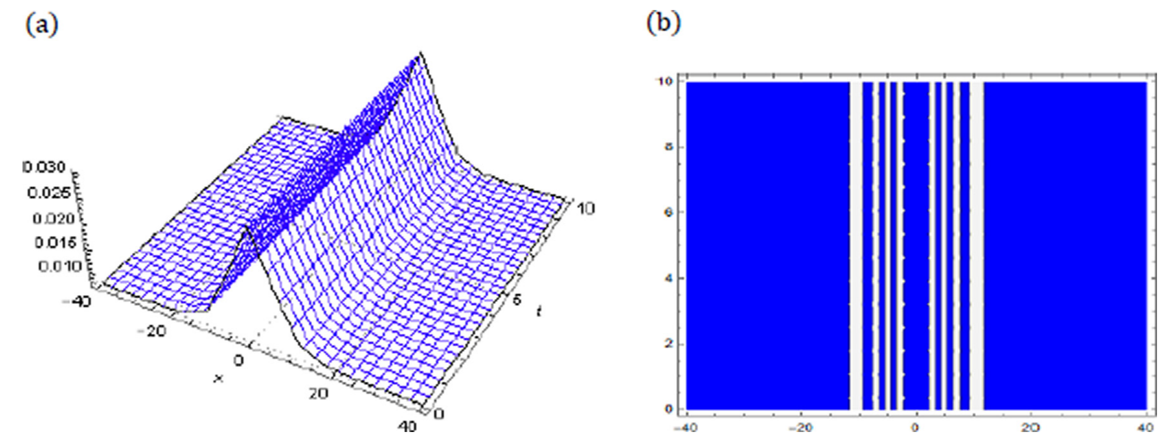

Fig. 7 Water wave profile of time-fractional Kaup-Kupershmidt model (97–98) with $\lambda = 0.1$, $\mu = 0$, $\omega = 1$, and $\alpha = 0.75$: (a) surface plot of $\upsilon_3(x, t)$ and (b) contour plot of $\upsilon_3(x, t)$.

Table 5 Comparison of absolute error of fractional Kaup-Kupershmidt model (97–98) at $\lambda = 0.1$, $\mu = 0$, $\omega = 1$, and $\alpha = 0.75$.

x_i	$t = 0.1$			$t = 0.3$		
	FCRPSA	LMM [33]	OHAM [33]	FCRPSA	LMM [33]	OHAM [33]
0.1	3.4695×10^{-18}	3.5268×10^{-10}	3.4968×10^{-10}	2.7322×10^{-17}	1.0519×10^{-9}	6.5846×10^{-9}
0.3	3.9031×10^{-18}	1.0532×10^{-9}	2.6793×10^{-5}	2.6888×10^{-17}	3.1535×10^{-9}	2.6651×10^{-5}
0.5	3.0358×10^{-18}	1.7520×10^{-9}	1.0061×10^{-4}	2.7756×10^{-17}	5.2500×10^{-9}	1.0037×10^{-4}
0.7	3.4695×10^{-18}	2.4480×10^{-9}	2.1579×10^{-4}	2.7756×10^{-17}	7.3381×10^{-9}	2.1549×10^{-4}
0.9	3.0358×10^{-18}	3.1402×10^{-9}	3.6399×10^{-4}	2.7756×10^{-17}	9.4146×10^{-9}	3.6370×10^{-4}
x_i	$t = 0.7$			$t = 0.9$		
	FCRPSA	LMM [33]	OHAM [33]	FCRPSA	LMM [33]	OHAM [33]
0.1	1.5049×10^{-16}	2.4259×10^{-9}	1.4638×10^{-8}	2.4893×10^{-16}	3.1007×10^{-9}	1.6457×10^{-8}
0.3	1.5049×10^{-16}	7.3297×10^{-9}	2.6372×10^{-5}	2.4893×10^{-16}	9.4057×10^{-9}	2.6235×10^{-5}
0.5	1.5092×10^{-16}	1.2222×10^{-8}	9.9885×10^{-5}	2.4850×10^{-16}	1.5695×10^{-8}	9.9643×10^{-5}
0.7	1.5005×10^{-16}	1.7094×10^{-8}	2.1491×10^{-4}	2.4720×10^{-16}	2.1960×10^{-8}	2.1461×10^{-4}
0.9	1.4962×10^{-16}	2.1939×10^{-8}	3.6312×10^{-4}	2.4676×10^{-16}	2.8191×10^{-9}	3.6282×10^{-4}

Sawada-Kotera, Lax's Korteweg-de Vries, Caudrey-Dodd-Gibbon, and Kaup-Kupershmidt equations. Based on time-conformable residual functions, MTFS solutions have been investigated without imposing any unjustified restrictions or linearization on the structure of the presented problems. The efficiency and accuracy of the proposed technique have been accomplished by numerical applications. The theoretical framework is supported via 2D and 3D graphical representation of some obtained solutions in limited domains of spatial and temporal variables that were depicted to visualize dynamic behavior as well, which relies noticeably on time. A comparison between our results and other existing numerical results is discussed and the calculations and simulations have been introduced with the aid of Mathematica 10. Conclusively, acquiring analytical solutions for different kinds of time-FNEEs is a difficult undertaking, encouraging further studies to obtain solutions to these models under an FCD of a fractional order bigger than one. Ideally, this investigation will be helpful to analysts, later on, to manage complex spacetime time-FPDEs in higher dimensions.

Declaration of Competing Interest

The authors declare that they have no known competing financial interests or personal relationships that could have appeared to influence the work reported in this paper.

Acknowledgment

The authors would like to express their gratitude to the unknown referees for carefully reading the paper and their helpful comments.

Funding

Not Applicable.

Availability of data and materials

Not Applicable.

Author's contributions

All authors carried out the proofs and conceived of the study. All authors read and approved the final manuscript.

References

[1] M. Ito, An extension of nonlinear evolution equations of the K-dV (mK-dV) type to higher orders, J. Phys. Soc. Jpn. 49 (2) (1980) 771–778.
[2] C.T. Lee, Some remarks on the fifth-order KdV equations, Math. Anal. Appl. 425 (1) (2015) 281–294.
[3] C. Liu, Z. Dai, Exact soliton solutions for the fifth-order Sawada-Kotera equation, Appl. Math. Comput. 206 (1) (2008) 272–275.
[4] A.R. Adem, X. Lü, Travelling wave solutions of a two-dimensional generalized Sawada-Kotera equation, Nonlinear Dyn. 84 (2) (2016) 915–922.
[5] M.T. Darvishi, F. Khani, Numerical and explicit solutions of the fifth-order Korteweg-de Vries equations, Chaos, Solitons Fractals 39 (5) (2009) 2484–2490.
[6] Y. Guo, D. Li, J. Wang, The new exact solutions of the Fifth-Order Sawada-Kotera equation using three wave method, Appl. Math. Lett. 94 (2019) 232–237.
[7] A.K. Gupta, S. Saha Ray, Numerical treatment for the solution of fractional fifth-order Sawada-Kotera equation using second kind Chebyshev wavelet method, Appl. Math. Model. 39 (17) (2015) 5121–5130.
[8] M. Al-Smadi, O. Abu Arqub, M. Gaith, Numerical simulation of telegraph and Cattaneo fractional-type models using adaptive reproducing kernel framework, Math. Methods Appl. Sci. 44 (10) (2021) 8472–8489.
[9] D. Baleanu, M. Inc, A. Yusuf, A.I. Aliyu, Lie symmetry analysis, exact solutions and conservation laws for the time fractional Caudrey-Dodd-Gibbon-Sawada-Kotera equation, Commun. Nonlinear Sci. Numer. Simul. 59 (2018) 222–234.
[10] M. Al-Smadi, O. Abu Arqub, Computational algorithm for solving fredholm time-fractional partial integrodifferential equations of dirichlet functions type with error estimates, Appl. Math. Comput. 342 (2019) 280-294.
[11] M. Al-Smadi, O. Abu Arqub, S. Momani, Numerical computations of coupled fractional resonant Schrödinger equations arising in quantum mechanics under conformable fractional derivative sense, Phys. Scr. 95 (2020) 075218.
[12] O.A. Arqub, N. Shawagfeh, Application of reproducing kernel algorithm for solving Dirichlet time-fractional diffusion-Gordon types equations in porous media, J. Porous Media 22 (4) (2019) 411–434.
[13] S. Kumar, A. Kumar, B. Samet, H. Dutta, A study on fractional host-parasitoid population dynamical model to describe insect species, Numerical Methods Partial Differential Equations 37 (2) (2021) 1673–1692.
[14] M. Inc, On numerical soliton solution of the Kaup-Kupershmidt equation and convergence analysis of the decomposition method, Appl. Math. Comput. 172 (1) (2006) 72–85.
[15] M. Al-Smadi, A. Freihat, O. Abu Arqub, N. Shawagfeh, A novel multistep generalized differential transform method for solving fractional-order Lu Chaotic and hyperchaotic systems, J Computational Analysis & Applications 19 (2015) 713–724.
[16] H. Dutta, A. Akdemir, A. Atangana, Fractional Order Analysis: Theory, Methods and Applications, Wiley, USA, 2020.
[17] O.A. Arqub, The reproducing kernel algorithm for handling differential algebraic systems of ordinary differential equations, Math. Methods Appl. Sci. 39 (15) (2016) 4549–4562.
[18] O. Abu Arqub, Solutions of time-fractional Tricomi and Keldysh equations of Dirichlet functions types in Hilbert space, Numer. Methods Partial Differential Equations 34 (5) (2018) 1759–1780.
[19] O. Abu Arqub, Fitted reproducing kernel Hilbert space method for the solutions of some certain classes of time-fractional partial differential equations subject to initial and Neumann boundary conditions, Comput. Math. Appl. 73 (6) (2017) 1243–1261.
[20] H. Günerhan, H. Dutta, M.A. Dokuyucu, W. Adel, Analysis of a fractional HIV model with Caputo and constant proportional Caputo operators, Chaos, Solitons Fractals 139 (2020) 110053.
[21] A. Atangana, D. Baleanu, New fractional derivatives with non-local and non-singular kernel: theory and application to heat transfer model, Thermal Science 20 (2016) 763–769.
[22] U. Afzal, N. Raza, I.G. Murtaza, On soliton solutions of time fractional form of Sawada-Kotera equation, Nonlinear Dyn. 95 (1) (2019) 391–405.
[23] O.S. Iyiola, A numerical study of Ito equation and Sawada-Kotera equation both of time-fractional type, Adv. Math.: Sci. J. 2 (2013) 71–79.
[24] J. Wang, T.-Z. Xu, G.-W. Wang, Numerical algorithm for time-fractional Sawada-Kotera equation and Ito equation with Bernstein polynomials, Appl. Math. Comput. 338 (2018) 1–11.
[25] O. Abu Arqub, Numerical solutions of systems of first-order, two-point BVPs based on the reproducing kernel algorithm, Calcolo 55 (2018) 1–28.
[26] O. Abu Arqub, Z. Odibat, M. Al-Smadi, Numerical solutions of time-fractional partial integrodifferential equations of Robin functions types in Hilbert space with error bounds and error estimates, Nonlinear Dyn. 94 (3) (2018) 1819–1834.
[27] A. Neamaty, B. Agheli, R. Darzi, Exact solution to time fractional fifth-order Korteweg-de Vries equation by using G''/G-expansion method, Acta Universitatis Apulensis 44 (2015) 21–37.
[28] S. Saha Ray, S. Sahoo, Two efficient reliable methods for solving fractional fifth order modified Sawada-Kotera equation appearing in mathematical physics, Journal of Ocean, Eng. Sci. 1 (3) (2016) 219–225.
[29] O. Abu Arqub, M. Al-Smadi, Numerical algorithm for solving time-fractional partial integrodifferential equations subject to initial and Dirichlet boundary conditions, Numer. Methods Partial Differential Equations 34 (5) (2018) 1577–1597.
[30] O. Abu Arqub, N. Shawagfeh, Solving optimal control problems of Fredholm constraint optimality via the reproducing kernel Hilbert space method with error estimates and convergence analysis, Mathematical Methods in the Applied Sciences (2019, 2019,) 1–18.
[31] M.S. Osman, D. Baleanu, A.R. Adem, K. Hosseini, M. Mirzazadeh, M. Eslami, Double-wave solutions and Lie symmetry analysis to the (2+ 1)-dimensional coupled Burgers equations, Chin. J. Phys. 63 (2020) 122–129.
[32] J.G. Liu, M.S. Osman, A.M. Wazwaz, A variety of nonautonomous complex wave solutions for the (2+ 1)-dimensional nonlinear Schrödinger equation with variable coefficients in nonlinear optical fibers, Optik 180 (2019) 917–923.
[33] M.S. Osman, H. Rezazadeh, M. Eslami, A. Neirameh, M. Mirzazadeh, Analytical study of solitons to benjamin-bona-mahony-peregrine equation with power law nonlinearity by using three methods, University Politehnica of Bucharest Scientific Bulletin-Series A-Applied Mathematics and Physics 80 (4) (2018) 267–278.
[34] Y. Ding, M.S. Osman, A.M. Wazwaz, Abundant complex wave solutions for the nonautonomous Fokas-Lenells equation in presence of perturbation terms, Optik 181 (2019) 503–513.
[35] K. Hosseini, M.S. Osman, M. Mirzazadeh, F. Rabiei, Investigation of different wave structures to the generalized third-order nonlinear Scrödinger equation, Optik 206 (2020) 164259.

[36] K.K. Ali, C. Cattani, J.F. Gómez-Aguilar, D. Baleanu, M.S. Osman, Analytical and numerical study of the DNA dynamics arising in oscillator-chain of Peyrard-Bishop model, Chaos, Solitons Fractals 139 (2020) 110089.
[37] K. Wajdi, H. Almusawa, S.M. Mirhosseini-Alizamini, M. Eslami, H. Rezazadeh, M.S. Osman, Optical soliton solutions for the coupled conformable Fokas-Lenells equation with spatio-temporal dispersion, Results Phys. 26 (2021) 104388.
[38] A. Akbulut, H. Almusawa, M. Kaplan, M.S. Osman, On the Conservation Laws and Exact Solutions to the (3+ 1)-Dimensional Modified KdV-Zakharov-Kuznetsov Equation, Symmetry 13 (5) (2021) 765.
[39] S. Djennadi, N. Shawagfeh, M.S. Osman, J.F. Gómez-Aguilar, O.A. Arqub, The Tikhonov regularization method for the inverse source problem of time fractional heat equation in the view of ABC-fractional technique, Phys. Scr. 96 (2021) 094006.
[40] H.O. Bakodah, Modified Adomian Decomposition method for the generalized fifth order KdV equations, Am. J. Comput. Math. 3 (2013) 53–58.
[41] H. Ahmad, T.A. Khan, P.S. Stanimirovic, I. Ahmad, Modified variational iteration technique for the mumerical solution of fifth order KdV-type equations, J. Appl. Comput. Mech. 6 (2020) 1220–1227.
[42] A.K. Gupta, S.S. Ray, The comparison of two reliable methods for accurate solution of time-fractional Kaup-Kupershmidt equation arising in capillary gravity waves, Math. Methods Appl. Sci. 39 (3) (2016) 583–592.
[43] M. Alabedalhadi, M. Al-Smadi, S. Al-Omari, D. Baleanu, S. Momani, Structure of optical soliton solution for nonliear resonant space-time Schrödinger equation in conformable sense with full nonlinearity term, Phys. Scr. 95 (2020) 105215.
[44] R.M. Jena, S. Chakraverty, S.K. Jena, H.M. Sedighi, On the wave solutions of time-fractional Sawada-Kotera-Ito equation arising in shallow water, Math. Methods Appl. Sci. 44 (1) (2021) 583–592.
[45] O. Abu Arqub, M. Al-Smadi, An adaptive numerical approach for the solutions of fractional advection-diffusion and dispersion equations in singular case under Riesz's derivative operator, Physica A 540 (2020) 123257, https://doi.org/10.1016/j.physa:2019.123257.
[46] O. Abu Arqub, Numerical solutions for the Robin time-fractional partial differential equations of heat and fluid flows based on the reproducing kernel algorithm, Int. J. Numer. Meth. Heat Fluid Flow 28 (4) (2018) 828–856.
[47] S. Djennadi, N. Shawagfeh, O. Abu Arqub, A fractional Tikhonov regularization method for an inverse backward and source problems in the time-space fractional diffusion equations, Chaos, Solitons Fractals 150 (2021) 111127.
[48] S. Djennadi, N. Shawagfeh, M. Inc, M.S. Osman, J.F. Gómez-Aguilar, O. Abu Arqub, The Tikhonov regularization method for the inverse source problem of time fractional heat equation in the view of ABC-fractional technique, *Physica Scripta* 96 (2021) 094006.
[49] S. Djennadi, N. Shawagfeh, O.A. Arqub, Well-posedness of the inverse problem of time fractional heat equation in the sense of the Atangana-Baleanu fractional approach, Alexandria Eng. J. 59 (4) (2020) 2261–2268.
[50] O.A. Arqub, M. Al-Smadi, N. Shawagfeh, Solving Fredholm integro-differential equations using reproducing kernel Hilbert space method, Appl. Math. Comput. 219 (17) (2013) 8938–8948.
[51] N. Shawagfeh, O. Abu Arqub, S. Momani, Analytical solution of nonlinear second-order periodic boundary value problem using reproducing kernel method, J. Comput. Anal. Appl. 16 (2014) 750–762.
[52] O. Abu Arqub, M. Al-Smadi, Atangana-Baleanu fractional approach to the solutions of Bagley-Torvik and Painlevé equations in Hilbert space, Chaos, Solitons Fractals 117 (2018) 161–167.
[53] O.A. Arqub, B. Maayah, Numerical solutions of integrodifferential equations of Fredholm operator type in the sense of the Atangana-Baleanu fractional operator, Chaos, Solitons Fractals 117 (2018) 117–124.
[54] O.A. Arqub, B. Maayah, Fitted fractional reproducing kernel algorithm for the numerical solutions of ABC–Fractional Volterra integro-differential equations, Chaos, Solitons Fractals 126 (2019) 394–402.
[55] O. Abu Arqub, B. Maayah, Modulation of reproducing kernel Hilbert space method for numerical solutions of Riccati and Bernoulli equations in the Atangana-Baleanu fractional sense, Chaos, Solitons Fractals 125 (2019) 163–170.
[56] R. Khalil, M. Al Horani, A. Yousef, M. Sababheh, A new definition of fractional derivative, J. Comput. Appl. Math. 264 (2014) 65–70.
[57] T. Abdeljawad, On conformable fractional calculus, J. Comput. Appl. Math. 279 (2015) 57–66.
[58] M. Al-Smadi, O. Abu Arqub, S. Hadid, An attractive analytical technique for coupled system of fractional partial differential equations in shallow water waves with conformable derivative, Commun. Theor. Phys. 72 (2020) 085001.
[59] O. Abu Arqub, M. Al-Smadi, Fuzzy conformable fractional differential equations: novel extended approach and new numerical solutions, Soft. Comput. 24 (2020) 12501–12522.
[60] M. Al-Smadi, O. Abu Arqub, S. Hadid, Approximate solutions of nonlinear fractional Kundu-Eckhaus and coupled fractional massive Thirring equations emerging in quantum field theory using conformable residual power series method, Phys. Scr. 95 (2020) 105205.
[61] D.R. Anderson, D.J. Ulness, Newly Defined Conformable Derivatives, Adv. Dynamical Syst. Appl. 10 (2015) 109–137.
[62] C. Chen, Y.-L. Jiang, Simplest equation method for some time-fractional partial differential equations with conformable derivative, Comput. Math. Appl. 75 (8) (2018) 2978–2988.
[63] Abu Arqub, Series solution of fuzzy differential equations under strongly generalized differentiability, J. Adv. Res. Appl. Math. 5 (1) (2013) 31–52.
[64] M. Al-Smadi, O.A. Arqub, D. Zeidan, Fuzzy fractional differential equations under the Mittag-Leffler kernel differential operator of the ABC approach: theorems and applications, Chaos, Solitons Fractals 146 (2021) 110891, https://doi.org/10.1016/j.chaos.2021.110891.
[65] M. Yavuz, B. Yaşkıran, Conformable derivative operator in modelling neuronal dynamics, Appl. Appl. Math.: Int. J. 13 (2018) 803–817.
[66] M. Yavuz, Novel solution methods for initial boundary value problems of fractional order with conformable differentiation, Int. J. Optimization Control: Theories Appl. 8 (2018) 1–7.
[67] B. Yaşkıran, M. Yavuz, Approximate-analytical solutions of cable equation using conformable fractional operator, New Trends Math. Sci. 5 (2017) 209–219.
[68] M. Yavuz, Dynamical behaviors of separated homotopy method defined by conformable operator, Konuralp, J. Math. 7 (2019) 1–6.
[69] M. Yavuz, A. Yokus, Analytical and numerical approaches to nerve impulse model of fractional-order, Numer. Methods Partial Differential Equations 36 (6) (2020) 1348–1368.